

# Toward Bionic Arthroscopy: A Comprehensive Perspective of Continuum Robotics Principles and Prototypes for the Inception of Arthroscopic Surgery Robots

Hao Huang, Zhenyun Shi, Xiangsheng Gao, Jian Zhou, Tengbo Yu, Chaozong Liu,\*  
Ziyu Liu, and Yingze Zhang

In this study, an innovative exploration of leveraging bionics and continuum robotics principles to develop a novel solution for arthroscopic surgery is embarked on. Inspired by the flexibility and adaptability of organisms like snakes and octopuses, the continuum robot concept aims to address the inherent challenges in traditional arthroscopy, including lower precision, manual tremors, and long surgeon learning curves. The implementation of these principles in the human body, however, faces significant obstacles, particularly achieving high-performance motion control amid strong nonlinearity and coupling between modules. This research focuses on intelligent integration and enhanced safety in human-machine interaction, aiming for improved control precision and flexibility in arthroscopic procedures. A thorough literature review of endoscopic continuum robots is conducted, highlighting current advancements in actuation, structure, sensing, and control technologies. The study concludes with an assessment of these technologies, their limitations, and future potential, in light of the unique demands of arthroscopic continuum robots. This comprehensive review bridges bionics and robotics, presenting the opportunities and challenges in applying continuum robotics to arthroscopic surgery. The goal is to encourage further research in this area, contributing to the development of prototype robots that enhance the precision and safety of arthroscopic surgery.


## 1. Introduction

Joints refer to the parts that connect two or more bones and their main function is to enable relative movement between bones. The human body has multiple joints, including the temporomandibular joint, shoulder joint, elbow joint, wrist joint, hip joint, knee joint, and ankle joint.<sup>[1]</sup> Joints are essential structures in the human body but are also prone to diseases. Common joint diseases include osteoarthritis, rheumatoid arthritis, and dislocations. According to data from the 2021 Global Rheumatoid Arthritis Network and the 2020 Centers for Disease Control and Prevention, over 350 million people worldwide suffer from arthritis.<sup>[2]</sup> Surgical treatment methods for osteoarthritis include arthroscopy and joint replacement surgery, where arthroscopy can clean the inflammatory tissue within the joint and relieve pain.<sup>[3]</sup>

Arthroscopy is a minimally invasive diagnostic and therapeutic procedure for joints, performed through a small incision on the skin. It is most commonly performed on the knee joint,<sup>[4]</sup> shoulder joint,<sup>[5]</sup> elbow joint,<sup>[6,7]</sup> wrist joint,<sup>[8,9]</sup> ankle joint,<sup>[10–13]</sup>

H. Huang, Z. Liu  
Beijing Advanced Innovation Centre for Biomedical Engineering  
School of Engineering Medicine  
Beihang University  
Beijing 100191, China

H. Huang, Z. Shi  
School of Mechanical Engineering and Automation  
Beihang University  
Beijing 100191, China

 The ORCID identification number(s) for the author(s) of this article can be found under <https://doi.org/10.1002/aisy.202300614>.

© 2023 The Authors. Advanced Intelligent Systems published by Wiley-VCH GmbH. This is an open access article under the terms of the Creative Commons Attribution License, which permits use, distribution and reproduction in any medium, provided the original work is properly cited.

DOI: 10.1002/aisy.202300614

X. Gao, C. Liu, Z. Liu  
Division of Surgery & Interventional Science  
University College London, Royal National Orthopaedic Hospital  
Stanmore HA7 4LP, UK  
E-mail: Chaozong.liu@ucl.ac.uk

J. Zhou, T. Yu, Z. Liu  
Qingdao Hospital  
University of Health and Rehabilitation Sciences (Qingdao Municipal Hospital)  
Qingdao 266071, China

T. Yu  
Department of Orthopaedic Surgery  
The Third Hospital of Hebei Medical University  
NO.139 Ziqiang Road, Shijiazhuang 050051, Hebei, China

Y. Zhang  
Affiliated Hospital of Qingdao University  
Qingdao, China

finger joints,<sup>[5,14,15]</sup> or hip joint.<sup>[16–18]</sup> Endoscopic science began with the Lichtleiter developed by Phillip Bozzini (1779–1809) in 1806, but it wasn't until 1912 that the endoscope was used in joints, proposed by Severin Nordentoft (1866–1922).<sup>[17]</sup> Arthroscopy is a mature minimally invasive surgery for diagnosing and treating joint diseases and injuries, such as knee arthroscopy, which costs the global healthcare system over 15 billion dollars annually.<sup>[19]</sup> During manually operated arthroscopic surgery, doctors use various tools and equipment to manipulate the structures inside the joint. Although arthroscopic surgery is more minimally invasive than traditional open surgery, it may still encounter the following problems<sup>[19]</sup>: 1) bleeding, injury, and infection; 2) lack of depth perception and limited field of view; 3) hand–eye coordination issues with the intraoperative field of view. These issues make the learning curve for arthroscopic surgery quite steep. For example, a report from the University of Oxford shows that doctors need to complete 170 cases to reach basic capabilities in knee arthroscopy.<sup>[20]</sup>

These issues stem from the inherent limitations of manual operations, including lower precision, manual tremors, lower dexterity of manual arthroscopes, and difficulty in maintaining sterility. The complexity of arthroscopic surgery results in a relatively long learning curve for surgeons, which may lead to accidents during surgery and postoperative complications. Advances in robotics and imaging technologies can alleviate these drawbacks and ease some of the healthcare system's access and workforce pressures.<sup>[19]</sup> Compared to traditional surgical approaches, arthroscopic robots can mitigate the impact of human factors on surgical outcomes and effectively reduce surgical risks. Additionally, arthroscopic robots offer advantages such as precise positioning, intelligent navigation, and dexterous obstacle avoidance, thereby enhancing surgical efficiency, accuracy, and providing better treatment outcomes and surgical experiences for patients. Therefore, the development of a high-precision, anti-tremor, highly dexterous, and intelligent arthroscopic robot holds significant potential.

Inspired by the bodies of snakes, elephant trunks, and octopus tentacles, continuum robots have been designed to structurally mimic their inherent agility and adaptability.<sup>[21]</sup> Compared with

traditional rigid-link manipulators, “continuum” mechanisms generate bending motion using a series of continuous arcs.<sup>[22]</sup> This design was initially focused on large-scale grasping, movement, and positioning in industrial applications,<sup>[22]</sup> even in enclosed environments for urban search and rescue operations.<sup>[23]</sup> The flexibility of continuum robots is suitable for surgical applications, achieving infinite degrees of freedom (DoF) operation within a small range, thereby reducing invasiveness to patients.<sup>[24–26]</sup> In addition to the robot's structure, an appropriate controller and corresponding sensors are also necessary conditions to ensure precise control performance.

**Figure 1a–c** illustrates the basic differences between 1) rigid-link, 2) hyper-redundant, and 3) continuum robots.<sup>[22]</sup> Compared with rigid-link and hyper-redundant robots, continuum robots use movement mechanisms similar to biological organs such as octopus tentacles and elephant trunks, using elastic deformation to make the flexible body bend into a smooth continuous curve to generate motion.<sup>[27]</sup> Figure 1d compares the basic performance of rigid-link robots and continuum robots from four factors: flexibility, position perception, operability, and load performance.<sup>[28]</sup> For the high-safety interaction and high-flexibility requirements of arthroscopy robots, continuum robots, due to their compliance and safety interaction characteristics, become a potential robot configuration feasible plan. However, the application of continuum robot technology to surgical instruments inside the human body is still in its infancy.

Integrating a continuum robot system into small-scale systems like arthroscopy presents some challenges. First, the space occupied by drive, sensing, and structural components must be minimized to make room for the robot's internal tool channel to accommodate surgical instruments and endoscopes. Second, under high compactness and actuation–sensing–structure integration, high-performance motion control for continuum robots is achieved with strong nonlinearity and strong coupling between modules. The following will discuss the actuation, structure, sensing, and control aimed at the needs of arthroscopic surgery robots, to realize intelligent integration, high human–machine interaction safety, high control precision, and flexibility of the arthroscopic surgery robot scheme.

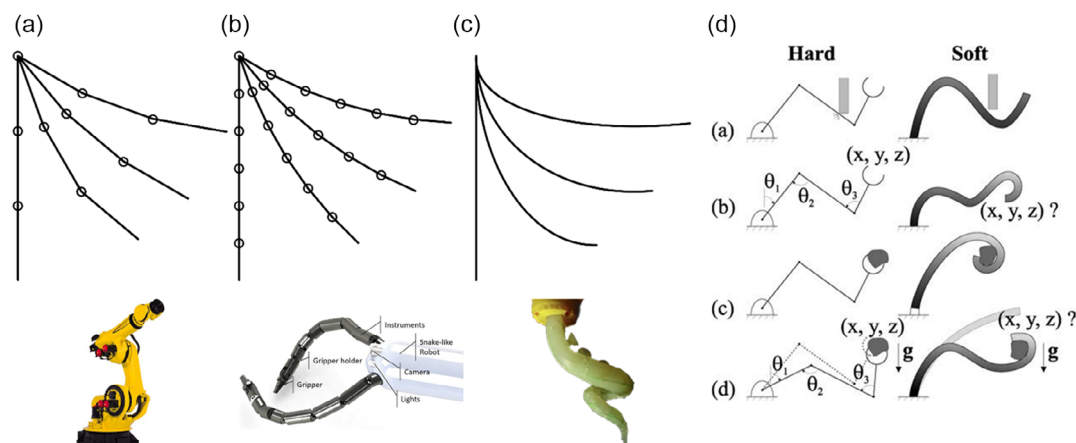


**Figure 1.** Comparison of three types of robots and performance comparison between rigid and continuum robots. a) Rigid-link robot;<sup>[300]</sup> b) hyper-redundant robot. Reproduced with permission.<sup>[172]</sup> Copyright 2018, Springer; c) continuum robot. Reproduced with permission.<sup>[301]</sup> Copyright 2019, Wiley; and d) performance comparison between rigid-link and continuum robots. Reproduced with permission.<sup>[28]</sup> Copyright 2008, Hindawi.

## 2. Actuation and Structure Design

### 2.1. Actuation

Although existing literature divides the actuation of continuum robots into two main categories, namely extrinsic and intrinsic,<sup>[29]</sup> the commonly used actuation methods can be roughly categorized into three types: underactuation based on cable length variation (cable-driven), pressure-driven based on fluid (fluid-driven), and deformation-driven based on smart materials (smart material-driven).

#### 2.1.1. Wire-Driven

Wire-driven continuum robots employ cables (such as shape memory alloy [SMA] wires and ropes) that are pulled by motors. The basic principle involves threading the cables through fixed points on the mechanical body of the robot. By pulling the cables at the root, a bending moment is generated at the fixed points, thereby causing bending deformation of the robot body.<sup>[30]</sup> To reduce the volume of the robot body, the actuation devices are usually placed on the robot base. However, cable-driven systems, which are driven by motors and transmission mechanisms, are complex and difficult to miniaturize and integrate.<sup>[31–33]</sup>

#### 2.1.2. Fluid-Driven

Pressure-driven based on fluid can be categorized into hydraulic and pneumatic actuation methods. Liquids have good compressibility, high-response frequency, and no loss when there is no leakage, making them promising for actuation in continuum robots.<sup>[34]</sup> Pneumatic actuation is widely used in continuum robots due to the advantages of lightweight medium, wide availability, and pollution-free properties. Pneumatic continuum robots typically control the expansion and contraction of pneumatic joints by changing the pressure of compressed air, thereby controlling the robot's motion. The traditional implementation involves storing air using a compressed air pump and changing the airflow direction using electromagnetic (EM) valves. This approach is not only used for driving pneumatic muscles and elephant trunk robots but also in hyperelastic silicone material robots. However, this method is bulky and consumes a large amount of air, which greatly limits the application of continuum robots in unstructured environments. To expand the application range of robots, researchers have made many improvements in pneumatic systems.<sup>[35–37]</sup>

#### 2.1.3. Smart Material-Driven

Smart materials are integrated into the robot body and controlled to deform under the effect of field effects such as electric fields, thermal fields, magnetic fields, or light, enabling the integration of the driving structure of the robot. Currently, SMAs are mostly used as smart materials for actuating continuum robots. SMA-driven continuum robots achieve motion by electrically heating the SMA to cause contraction. For example, when heated, SMA can recover its original shape. By embedding SMA into the robot body, the robot can be driven to move in a certain direction.<sup>[38,39]</sup>

Dielectric elastomers embedded in the robot body can drive complex movements by controlling their deformation under an electric field.<sup>[40–42]</sup> Magnetorheological elastomers used as robot bodies can drive robot motion by changing the intensity and direction of the magnetic field.<sup>[43]</sup> Ionic polymer–metal composites applied to robots can change the deformation direction of the material by applying voltage.<sup>[44]</sup> Furthermore, the recent advancements in liquid crystal elastomers (LCEs) provide a significant breakthrough, particularly for light-activated actuation in robotics.<sup>[45–47]</sup> These LCEs can undergo substantial elongation and contraction in response to light exposure, offering a unique approach to biomimetic movement in robotic systems.

#### 2.1.4. Hybrid Actuation

Hybrid-driven continuum robots generally combine multiple actuation methods mentioned earlier, such as pneumatic and cable-driven,<sup>[48]</sup> to achieve better performance, although control modeling becomes more complex.

#### 2.1.5. Other Actuation Methods

Some scholars have also employed unconventional actuation methods, such as water-jet-driven<sup>[49–51]</sup> and magnetic-driven,<sup>[52–54]</sup> each with its own limitations in specific application scenarios.

Among these actuation methods, fluid-driven often produces large noise due to the pump and has lower operating precision. Smart material-driven has lower response frequency due to temperature field or other field control. Therefore, wire-driven is often considered a feasible solution for arthroscopic surgery scenes with high-response frequency and high human–machine interaction safety.

## 2.2. Structure Design

Through the classification based on the material stiffness of the structural components that compose a robot, the structural continuum can be divided into two categories: soft continuum and rigid continuum. Soft continuum robots belong to the category of soft robots,<sup>[55–58]</sup> but their driving forms and structural designs are not suitable for minimally invasive endoscopic surgical robots with small outer diameters.

Rigid continuum structures refer to the mode of force and torque transmission directly through rigid elements.<sup>[59]</sup> Driven by the demand for high flexibility and small scale in medical intervention surgeries, there has been a great deal of innovation in the design of rigid continuum robots,<sup>[21,24,60]</sup> which can be classified as steerable needles,<sup>[61–63]</sup> concentric tubes,<sup>[64–68]</sup> notch tubes,<sup>[69–71]</sup> and backbone-based (hinged or continuous) robots.<sup>[30,72–75]</sup> **Figure 2** illustrates examples of implementations using these design principles.

#### 2.2.1. Design of Steerable Needles

Manipulable needles are usually made of flexible materials such as nitinol or other SMAs, which allow them to bend and curve while passing through tissues. The needle tip is typically

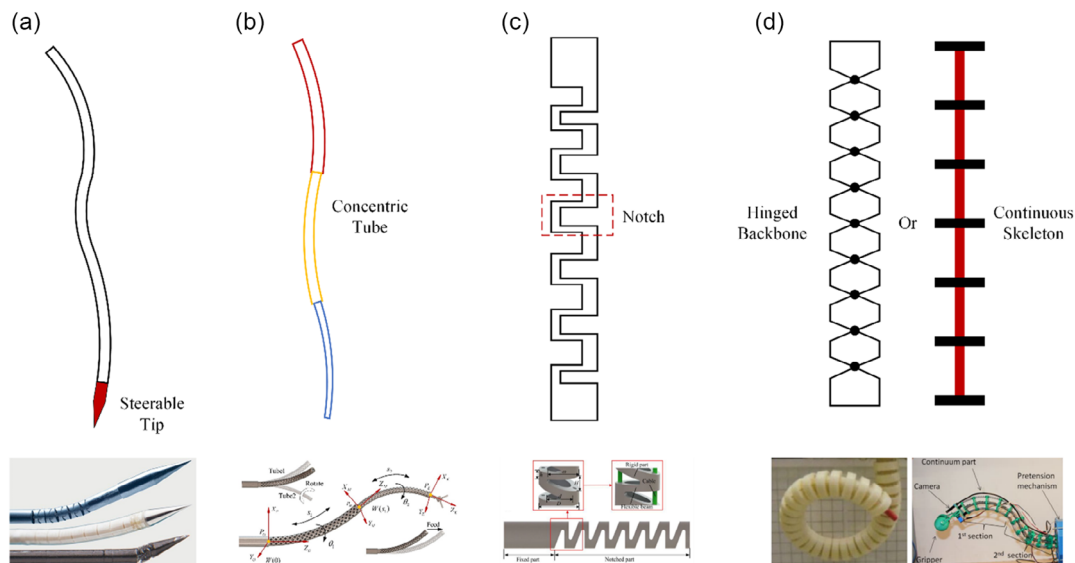


**Figure 2.** The demonstration of the designs of different continuum robots with rigid structures: a) steerable needle. Reproduced with permission.<sup>[302]</sup> Copyright 2018, Talory & Francis, b) typical concentric tube design. Reproduced with permission.<sup>[68]</sup> Copyright 2023, MDPI, c) notched tube. Reproduced with permission.<sup>[71]</sup> Copyright 2022, MDPI, and d) skeleton-based design. Reproduced with permission.<sup>[30,73]</sup> Copyright 2013, Sage; 2022, MDPI.

asymmetrical, with a bevel or other shape that bends in a specific direction when force is applied. By controlling the direction and magnitude of this bending, the needle can be guided to specific targets inside the body. One of the key features of manipulable needles is their ability to minimize tissue deformation and damage during insertion. By allowing more precise positioning, these needles can reduce the risk of complications and improve patient outcomes.<sup>[76–78]</sup> Furthermore, there have been improvements in the design of steerable needles in terms of reducing needle hardness, using different driving forms, and other purposes.<sup>[63,79–81]</sup>

### 2.2.2. Design of Concentric Tubes

Concentric tubes are structures composed of two or more nested tubes with different diameters.<sup>[82,83]</sup> They can be used to manufacture needles with piecewise constant curvature (PCC) or more general shapes. When bent tubes are inserted into each other to form a needle, their common axes must conform to the interacting curvatures. By relative movement and rotation of the tubes, the curvature and total length of the needle can be changed. Concentric tube robots are devices that utilize this structure to create flexible and manipulable tools for minimally invasive surgery. They consist of multiple concentric tubes that can be manipulated independently or simultaneously to achieve various motions and configurations. The outer tubes provide structural support, while the inner tubes can be used for sensing, imaging, or manipulation. Concentric tube robots have several features that make them useful in medical applications. They can traverse complex anatomical structures with precision and flexibility, enabling less invasive surgeries and faster patient recovery times. They also have the advantage of a small footprint and ease of integration into existing surgical systems. Although concentric tube robots were initially used for general surgical applications,

subsequent improvements have been made for specific surgical scenarios.<sup>[84–88]</sup>

### 2.2.3. Design of Notch Tubes

Notch tubes refer to thin-walled tubes with specific notch patterns carved out.<sup>[89–91]</sup> The purpose of the notches is to enable bending of the thin-walled tubes. The materials commonly used for notch tubes are nitinol and polypropylene plastics. These notch tubes can be used as the backbone of a continuum and do not require intervertebral discs. Larger bending curvatures pose significant challenges for concentric tube continua. To maintain miniaturization and achieve large curvature bending, a new type of asymmetric notched concentric tube was introduced based on the design of concentric tubes.<sup>[92]</sup> Additionally, connecting multiple segmented notch tubes in series can achieve a multi-DoF continuum robot.<sup>[93]</sup>

### 2.2.4. Backbone-Based Design

Backbone-based continuum robot design refers to using a continuous or multi-joint hinged support backbone as the main structure of the robot.<sup>[88,94–97]</sup> This backbone support includes drive cables, sensors, and other components, and the skeleton provides a spring force for returning to its original position and can form curves with equal curvatures during driving. Scholars have used various structures to achieve such skeletons, such as springs,<sup>[75,98,99]</sup> polymers,<sup>[100]</sup> and nitinol rods/tubes.<sup>[74,96,101]</sup> Tendons or rods are wired along the length of the backbone, and when using a continuous skeleton, intervertebral discs fixed on the desired wiring path are required and fixed at specific distal points. In contrast, intervertebral discs are not necessary when using hinged structures. By continuously



stacking segments of this design, more DoF can be achieved. Figure 2d shows hinged and continuous backbone designs, with hinged structures often supplemented with elastic components to achieve bending and resilience of the continuum, while continuous structures can also be multi-segmented elastic skeleton structures.

### 2.2.5. Variable Stiffness

In practical applications, continuum robots also need to adjust their stiffness. Existing technical solutions include configurations with antagonistic tendons-fluidic bags,<sup>[33,102,103]</sup> pressure/vacuum interference techniques,<sup>[104,105]</sup> the use of SMAs,<sup>[99]</sup> or insertable constraints.<sup>[106]</sup>

Despite the advantages of rigid continuum robots, such as a wide range of motion and ease of configuration, the high level of hysteresis caused by internal friction and tension loss in the drive cables restricts their development, making it challenging to scale down these multi-segmented, variable-length, and adjustable-stiffness designs to a scale suitable for surgical applications.

## 3. Sensing

Arthroscopic surgery is a type of minimally invasive surgery. Continuum robots can perform precise operations on anatomical structures along curved paths through small incisions or natural orifices within the human body, relying on accurate perception of the continuum robot's body shape.<sup>[107]</sup> Due to the limitations of the structure used for minimally invasive surgical robots, it is challenging to apply traditional sensors such as encoders, potentiometers, strain gauges, and inertial measurement units (IMUs). There is an urgent need to develop new types of compatible, embeddable, and miniaturized sensors. This section explores the latest advancements in alternative emerging technologies for 3D shape sensing in this field, including methods for shape reconstruction based on flexible sensors, fiber-optic sensors, EM tracking, and intraoperative imaging modalities.<sup>[107,108]</sup>

### 3.1. Flexible Sensors

Flexible sensors are based on the principle that the resistance or capacitance of conductive smart materials changes under strain, allowing measurement of information such as bending, stretching, and stress.<sup>[109–113]</sup> Currently available commercial flexible sensors such as Flex Sensor, FlexiForce, Bend Sensor, and StretchSense possess certain flexibility and can be attached to or embedded in the continuum robot's body. However, the elastic modulus of these sensors can have an impact on the robot's own motion, and their models are fixed and difficult to customize or trim. To better adapt the sensors to the needs of continuum robots, scholars have explored new materials and processing techniques. For example, by injecting conductive liquid eutectic gallium–indium into microchannels within a silicone body, the resistance of the conductive liquid changes as the body deforms.<sup>[114,115]</sup> By altering the arrangement of the internal channels, information such as axial strain, pressure, and bending can be measured.<sup>[116,117]</sup> Flexible sensors are widely used in the field of continuum robots. In medical robots, for instance, flexible

sensors can be embedded in the robot's body to measure the bending state and force of surgical instruments during operations, thereby improving surgical quality and safety.

### 3.2. Fiber Bragg Grating

FBG sensors, short for fiber Bragg grating sensors, are a type of fiber-optic sensor.<sup>[118–120]</sup> They utilize the periodic variation of refractive index within the fiber core to reflect a specific wavelength known as the Bragg wavelength. The principle of FBG sensors is based on the wavelength variation of the reflected light, which is proportional to the strain or temperature experienced by the fiber. FBG sensors consist of an optical fiber segment with a periodic refractive index variation,<sup>[69,121–129]</sup> which is achieved through ultraviolet exposure.<sup>[130–135]</sup> The advantages of FBG sensors include high sensitivity, immunity to EM interference, and the ability to measure multiple parameters simultaneously. However, their disadvantages include high cost, limited dynamic range, and the need for specialized equipment for installation and decoding. FBG sensors find applications in structural health monitoring, aerospace, civil engineering, and biomedical sensing.

### 3.3. EM-Tracking-Based Sensors

EM-tracking sensors<sup>[136–145]</sup> utilize an EM field to track the position and orientation of objects.<sup>[146–150]</sup> These sensors can be embedded in any part of the robot's body<sup>[151]</sup> and serve as localization points within the task space. The advantages of EM-tracking sensors include high precision, fast response time, and the ability to operate in harsh environments. However, they are susceptible to interference from other EM sources and require calibration. EM-tracking sensors find wide applications in robotics, motion capture, medical imaging, and other fields.<sup>[152–160]</sup>

### 3.4. Vision-Based Shape-Sensing Techniques

Vision-based shape-sensing techniques capture images of the robot and its surrounding environment using cameras, and then reconstruct the shape of the robot using computer vision algorithms. These techniques are based on triangulation, involving the measurement of the robot's position from multiple camera perspectives.<sup>[161–164]</sup> The advantages of vision-based shape sensing include high accuracy, noninvasiveness, and real-time feedback capability. However, they are sensitive to lighting conditions and require calibration. Vision-based shape-sensing techniques are used in various applications, including robotics, medical imaging, and virtual reality.

Vision-based shape-sensing techniques include perspective-imaging-based shape reconstruction,<sup>[165–169]</sup> endoscope-based shape reconstruction,<sup>[147,148,170–177]</sup> and ultrasound-based shape reconstruction.<sup>[178–187]</sup> Perspective-imaging-based shape reconstruction techniques offer high accuracy and real-time feedback capabilities due to the use of X-rays, but they face challenges due to significant radiation exposure and the use of contrast agents. Endoscope-based shape reconstruction offers high accuracy, noninvasiveness, and real-time feedback capabilities. However, it is sensitive to lighting conditions and requires calibration.

Ultrasound-based shape reconstruction is a technique that estimates the shape of a surgical continuum robot using ultrasound imaging. Its advantages include noninvasiveness, real-time feedback, and the ability to operate in challenging environments. However, its limitations include limited accuracy and sensitivity to tissue properties.

Among these sensing methods, due to the 3D sensing requirements, real-time constraints, and volume limitations (5 mm outer diameter) of arthroscopic robots,<sup>[18]</sup> the application of 2D sensors, magnetic flux sensors, and microfluidic multi-axis force sensors is limited. FBG sensors, in contrast, are a feasible solution for arthroscopic continuum robots due to their high real-time capability, ability to sense 3D curvature, and their small diameter in the sub-millimeter range.

## 4. Control

To accurately approach the target detection area in arthroscopic surgery, navigation and control are also important aspects. However, the surgical route of arthroscopy is always narrow and constrained, the field of view of the endoscope at the tip of the continuum is limited, and the strong nonlinearity and uncertainty of the continuum robot itself pose considerable challenges to the development of highly compliant, high-frequency responsive, and high-precision control algorithms. This section first discusses the kinematics, dynamics, and model-free methods of continuum robots, and then addresses control patterns and related control theories.

### 4.1. Kinematics

Recent research<sup>[188]</sup> classifies the kinematics of infinite-DoF continuum robot into continuous kinematics, modal kinematics, and discrete kinematics based on the order reduction of system DoF. Continuous kinematics refers to the backbone of the robot being a continuously variable curvature curve,<sup>[94,189–192]</sup> often modeled using Cosserat rod theory. Continuous kinematics often employ inverse solutions using partial differential equations and ordinary differential equations, such as numerical iteration methods and optimization methods, to obtain inverse kinematics. Modal kinematics involve fitting the shape and strain of the robot using reduced-order models,<sup>[193–196]</sup> such as piecewise constant strain or curvature,<sup>[21]</sup> as well as using traditional rigid-link robot kinematics like the Denavit–Hartenberg (D–H) method to simulate the kinematic model of the continuum robot. Modal kinematics can use analytical and iterative methods similar to traditional rigid-link robotic arms to obtain the corresponding inverse kinematics. Discrete kinematics provide approximate values of robot kinematics using discrete rods, pseudo-rigid bodies, discrete elements, finite-element methods (FEMs), etc.<sup>[197–202]</sup> Inverse kinematics solutions for discrete kinematics can be obtained through inverse mapping relationships corresponding to the respective methods.

### 4.2. Dynamics

Dynamics is often built upon the foundation of the kinematic model. In this section, we will describe the dynamic models

of continuous kinematics, modal kinematics, and discrete kinematics based on their respective foundations. The establishment of dynamic models is to achieve motion control that kinematic models cannot achieve, such as high-speed motion, external force loading, and vibration compensation.<sup>[203]</sup> For continuous kinematics represented by the Cosserat rod theory, some scholars have proposed using the Lagrangian method to establish dynamic models<sup>[204]</sup> and designed a dynamic controller for continuum manipulators using Ritz and Ritz–Galerkin methods. This method assumes that the robot cross section does not deform, only the bending deformation of the robot’s centerline. The dynamics corresponding to modal kinematics can be established using similar methods as rigid-link robotic arms after system order reduction, such as Lagrangian and Newtonian methods.<sup>[205]</sup> Some scholars have used the D–H parameter method based on the PCC hypothesis to design dynamic controllers.<sup>[206,207]</sup> However, for discrete kinematics, calculating the dynamics using FEM numerical models consumes too much computing power and cannot achieve real-time dynamic control. To reduce computational costs, scholars have used model order-reduction methods and classical control theory to achieve simulation<sup>[208]</sup> and real robot control.<sup>[209–211]</sup>

### 4.3. Data-Driven Model

In addition to analytical model-based methods, researchers have also proposed data-driven machine-learning-based methods, such as supervised learning<sup>[212–220]</sup> and reinforcement learning.<sup>[221–229]</sup> Based on preexperimental kinematic and dynamic data, these methods use artificial neural networks trained with the data as black box models for kinematics and dynamics. The advantage of this black box model approach lies in its ability to handle strong nonlinearity and uncertainty that analytical models cannot address, without the need to establish theoretical models or perform experimental calibration. However, black box models are often not interpretable and rely on high-quality sensor data. The combination of analytical models and data-driven models is another trend in the control of continuum robots.<sup>[230–236]</sup> Although analytical methods pose challenges in parameter representation and modeling uncertainty, their solutions often converge and can be combined with online learning to leverage their respective advantages, including convergence performance, no need for prior exploration data, and online control error compensation.<sup>[237]</sup>

### 4.4. Motion Planning

The motion planning modes of continuum robots (see **Figure 3**) can often be divided into “Following the leader (FTL),” “Coiling,” and “Circumnutation”.<sup>[188]</sup> The motion pattern of circumnutation imitates the movements of vines and pea plants in nature.<sup>[238,239]</sup> It is designed to overcome the disadvantages of slender structures with low stiffness and provide motion support.<sup>[240]</sup> Coiling is more like the trunk of an elephant wrapping around a target object,<sup>[241]</sup> aiming to achieve stable grasping or coiling motions.<sup>[242–246]</sup> FTL mimics the motion of a snake.<sup>[247]</sup> Its purpose is to utilize the hyper-redundant or infinite DoF of the continuum robot to achieve

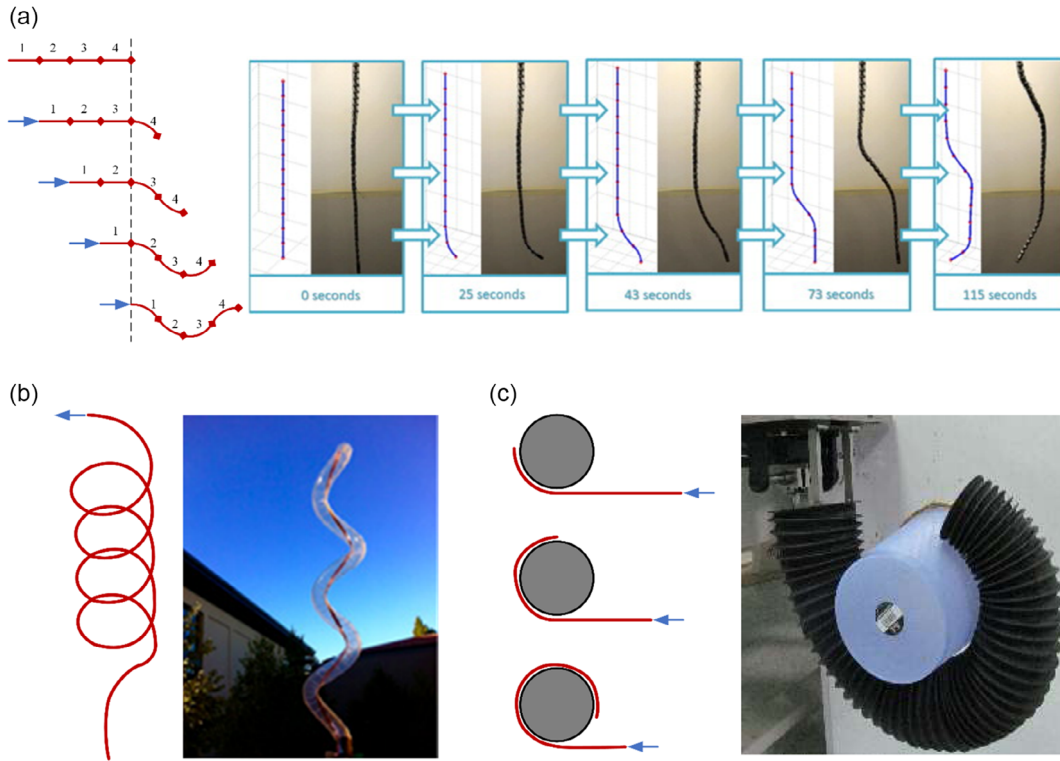


**Figure 3.** Three methods of continuum robot motion planning. Reproduced with permission.<sup>[188]</sup> Copyright 2023, Wiley: a) following the leader (FTL) navigation. Reproduced with permission.<sup>[247]</sup> Copyright 2014, Elsevier; b) a growing robot. Reproduced with permission.<sup>[240]</sup> Copyright 2017, The American Association for the Advancement of Science; and c) grasping objects like elephant trunk. Reproduced with permission.<sup>[242]</sup> Copyright 2019, American Society of Mechanical Engineers.

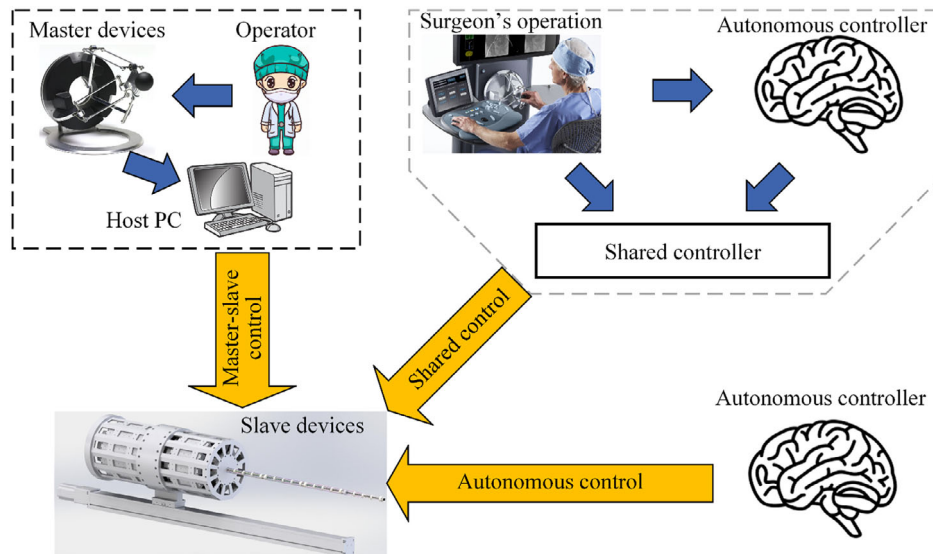


**Figure 4.** Illustration of the three control modes of the robot. Reproduced with permission.<sup>[303]</sup> Copyright 2021, Beihang University.

flexible obstacle avoidance movements.<sup>[97,248,249]</sup> Due to the limitations of arthroscopic surgery scenarios, the characteristics of the FTL motion pattern are more suitable for arthroscopic surgical robot applications.

#### 4.5. Control Pattern

Continuum robots for medical applications often adopt three control patterns (see **Figure 4**): master–slave control, shared

control, and autonomous control.<sup>[250]</sup> Master–slave control usually uses a master device (e.g., a joystick) as the input for control commands, with the continuum robot acting as the slave to execute the input control commands.<sup>[251–259]</sup> Shared control refers to using algorithms based on principles such as obstacle avoidance, improved compliance, and optimal efficiency to assist in controlling the motion of the continuum robot, building upon master–slave control.<sup>[260–263]</sup> Autonomous control, as the name suggests, allows the continuum robot to autonomously control its own motion to reach target positions and orientations.<sup>[21,59,194,264–267]</sup> Due to the small-diameter structure of arthroscopic surgery instruments, which is not conducive to installing sensors for external environment sensing, and the narrow and fragile workspace of the robot, a shared controller suitable for this scenario should be a key direction for development.

## 5. State-of-the-Art Continuum Robotics Technology for Endoscopic Application

Current arthroscopes, typically rigid with diameters ranging from 0.5 to 5 mm, facilitate direct observation of joint morphology and lesions by being inserted into the joint cavity through small skin incisions. This is exemplified in **Figure 5a**, which illustrates a standard arthroscopic system. However, the intricacy of joint structures often leads to blind spots or suboptimal clarity during inspections with rigid arthroscopes, hindering their ability to satisfy increasingly complex diagnostic requirements. **Figure 5b** demonstrates these limitations in the arthroscope’s operational scope. The integration of continuum robotics technology presents a promising solution to these challenges, signifying a progressive trend in the evolution of arthroscopic techniques. Due to the small-size design requirements and intelligent drive navigation demands of arthroscopic surgical robots, there are currently no reported designs of relevant continuum robots. In this section, we analyze the design of endoscope continuum robots with similar requirements to obtain similar demands and technological guidance for arthroscopic surgical robots. This chapter systematically reviews the research milestones of endoscope continuum robots from 2012 to the present.

The literature references used in this review were obtained from a search on Web of Science using the keywords “Endoscope” and “Continuum robot,” excluding all review articles. Focusing on the specific requirements of arthroscopic surgery, including the need for a tool channel inside the robot body and the requirement for a single-continuum robot instead of multiple parallel ones, we selected representative studies for in-depth analysis. The representative research articles are shown in **Table 1**.

Continuum robots, designed for endoscopic procedures, exhibit a broad applicability across various medical domains. Their utility extends to gastrointestinal tract endoscopy,<sup>[48,268,269]</sup> paranasal sinus surgery,<sup>[250]</sup> laryngeal interventions,<sup>[270]</sup> and maxillary sinus operations.<sup>[259]</sup> The typical structure and application scenarios are depicted in **Figure 6**. These robotic systems are generally composed of mechanical assemblies, cameras, endoscopes, and image display units. Despite their potential, continuum robots for endoscopy are yet to be clinically tested and currently remain in the preclinical phase, limited to specimen-based experimentation.

### 5.1. Structure

Among the four types of structures mentioned in Section 2.2, the backbone-based type is the most common due to the requirements of minimally invasive surgical endoscope scenarios, such as small outer diameter, high flexibility, easy interchangeability, and the presence of a tool channel. In addition to the backbone type, Butler et al.<sup>[271]</sup> proposed a structure combining concentric tubes and a backbone, while Gao et al. and Hong et al.<sup>[249,272]</sup> reported endoscope continuum robots using a notched tube structure. The concentric tube structure is less flexible and can easily cause tissue damage, while the notched tube structure, due to its structural characteristics, often achieves only single-DoF bending in each segment. In terms of outer diameter, the notched tube can achieve a smaller diameter than the backbone, enabling functionality in narrower workspaces, and it can have a larger proportion of tool channel cross-sectional area. In summary, for scenarios with extremely narrow spaces that require miniaturization but have relatively regular structures,

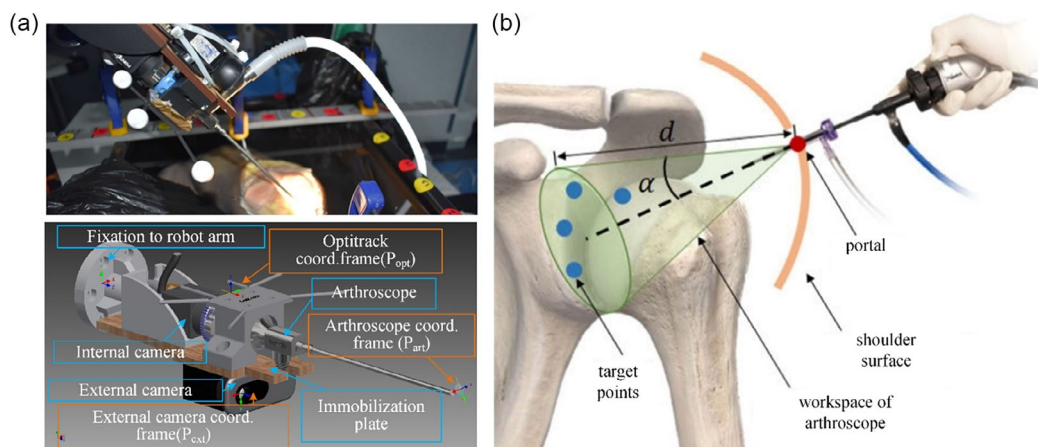


**Figure 5.** Composition of a typical arthroscope system: a) arthroscopic robot platform. Reproduced with permission.<sup>[304,305]</sup> Copyright 2019, IEEE; and b) workspace of arthroscope. Reproduced with permission.<sup>[306]</sup> Copyright 2021, IEEE.



**Table 1.** Technical specifications of endoscopic continuum robots in the past decade.

References/ year <sup>a)</sup>	Structural classification	Active segments/ degree of freedom	Single-section bending angle	Max diameter/tool channel diameter	Actuation method	Sensing technology	Control accuracy: end tip deviation/length	Modeling method	Motion planning	Control pattern
[271]/2012	Concentric tube; backbone	2 segments/3 DoFs	±180°	12 mm/φ 3.7 mm endoscope	Cable-driven	NM	NM/25 mm	Algebraic model	NM	NM
[283]/2014	Backbone	7 segments/14 DoFs	±180°	15 mm/4 mm	Cable-driven	Gyroscopes	52 mm/910 mm	Modal model	Uncoiling; FTL	Autonomous control
[286–288]/ 2015	Backbone	2 segments/2 DoFs	±90°	3.4 mm/1.4 mm	Cable-driven	NM	0.5 mm/120 mm	PCC model	NM	NM
[307]/2015	Backbone	1 segments/1 DoFs	±180°	10 mm/8 mm	Cable-driven	NM	NM/55 mm	NM	NM	NM
[289]/2016	Backbone	3 segments/6 DoFs	±45°	8 mm/φ 1.2 mm endoscope	Cable-driven	NM	3 mm/84 mm;	D–H model; iterative method	NM	NM
[308]/2016	Backbone	1 segments/2 DoFs	±180°	6.5 mm/2 mm	Cable-driven	NM	0.143% bending angle error/60 mm	CC model	NM	NM
[309]/2018	Backbone	3 segments/5 DoFs	NM	21 mm/NM	Cable-driven	NM	NM/260–340 mm	CC model	NM	NM
[292]/2019	Backbone	2 segments/6 DoFs	NM	About 10 mm/NM	Cable-driven	NM	NM/100–200 mm	CC model	FTL	NM
[268,278]/ 2019	Backbone	1 segments/3 DoFs	±80°	13.5 mm/NM	Fluid-driven	EM sensors	RMSE of bending angle is 7.76°/14–29 mm	CC model	NM	Master–slave control
[272]/2020	Notched tube	1 segments/1 DoF	090°	1.6 mm/1.4 mm	Cable-driven	NM	NM/3–15 mm	CC model	NM	NM
[249]/2020	Notched tube	6 segments/6 DoFs	Larger than ±180° for total length;	3.4 mm/1.8 mm	Cable-driven	NM	1.78 mm at 180° in C- shaped curve/60 mm	PCC model	FTL	Autonomous control
[53]/2020	Backbone	1 segments/2 DoFs	±90°	5 mm/NM	Magnetic- driven	Temperature sensor	NM/45 mm	Euler–Bernoulli beam model; CC model	NM	NM
[280,281]/ 2020	Backbone	2 segments/5 DoFs	±90°	11.5 mm/5.75 mm	Cable-driven	Vision-based sensors	0.25 mm/45 mm	NM	NM	Shared control
[49–51]/ 2020	Backbone	1 segments/2 DoFs	NM	10 mm/3.9 mm endoscope diameter	Water-jet actuators	IMU; EM sensors;	5.1 mm±2 mm/60 mm	Cosserat rod model	NM	Shared control
[284]/2020	Backbone	NM	NM	2.8 mm/φ 0.8 mm endoscope	NM	FBG sensors; EM sensors; force/torque sensors	NM/NM	Cosserat rod model; data- driven model;	NM	NM
[290]/2021	Backbone	1 segments/2 DoFs	±90°	5 mm/2 mm	SMA spring; cable-driven	EM sensors	1.15 mm/20 mm	CC model	NM	Master–slave control
[282]/2021	Backbone	1 segments/2 DoFs	±180°	10 mm/more than 2 mm	Cable-driven	Vision-based sensors	NM/60 mm	Data-driven model	NM	Autonomous control
[293]/2021	Backbone	3 segments/6 DoFs	NM	3.3 mm/2.1 mm	Cable-driven	NM	NM/50 mm	CC model	FTL	Master–slave control
[54]/2022	Backbone	4 segments/4 DoFs	NM	2 mm/NM	Magnetic- driven	Vision-based sensors	Heading error: 36.8°/80 mm	Magnetoelastic CR model	FTL	Autonomous control

<sup>a)</sup>Ref., references; NM, not mentioned; DoF, degrees of freedom; FTL, following the leader; CC, constant curvature; PCC, piecewise constant curvature; D–H, Denavit–Hartenberg; EM, electromagnetic; RMSE, root-mean-square error; IMU, inertial measurement unit; FBG, fiber Bragg grating; SMA, shape memory alloy; IK, inverse kinematics.

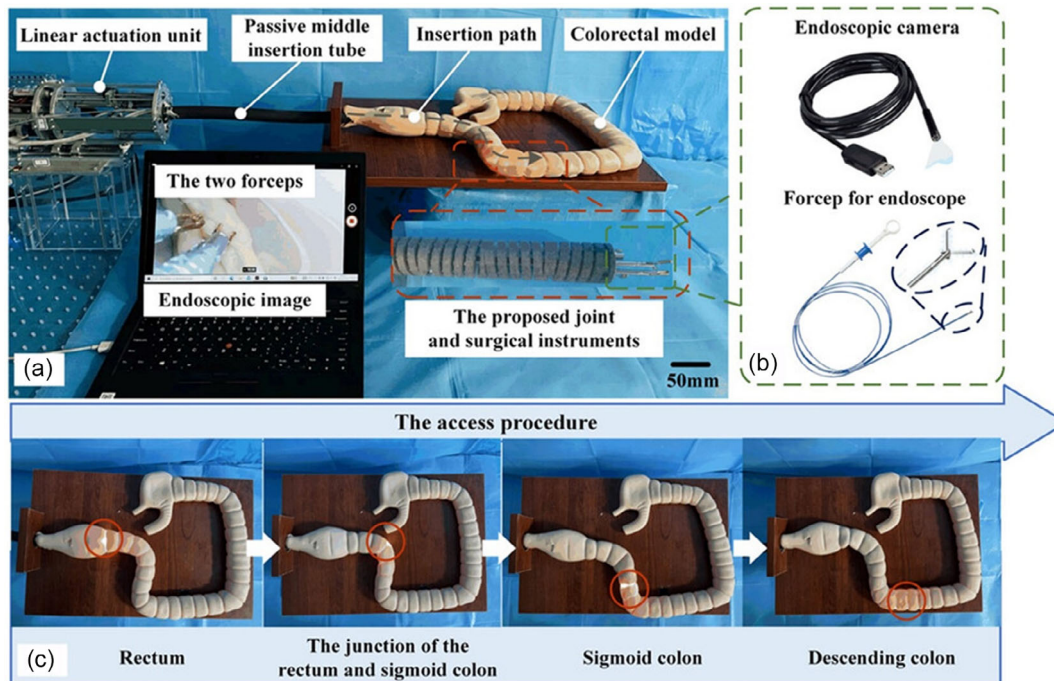


**Figure 6.** Illustration of the composition and applications of a typical endoscopic continuum robot system. Reproduced with permission.<sup>[48]</sup> Copyright 2023, Wiley: a) experimental setup for phantom testing; b) endoscopic camera and forceps employed in the experiment; and c) illustration of the insertion access process of the designed continuum joint (the red circle represents the actual position).

the notched tube structure may be more suitable. However, for workspaces with more complex requirements and less stringent outer diameter requirements, the backbone-type structure is more appropriate.

Building on prior research, scholars have persistently refined the structural parameters of robots to improve both their flexibility and stiffness. This advancement aims to better fulfill the specific demands of endoscopic applications. A strategy to boost the operational capabilities of continuous robots involves segmenting them into two parts and controlling each independently. Wang et al.<sup>[273]</sup> introduced a streamlined, compact soft robot with two segments. The robot's proximal segment (PS), powered hydraulically, provides omnidirectional bending to navigate toward lesions. Conversely, its distal segment (DS), tendon-driven, ensures precise and rapid steering of a laser collimator for targeted lesion treatment. Additionally, Hong et al.<sup>[259]</sup> unveiled a novel two-segment continuum robot designed for maxillary sinus surgery, as illustrated in **Figure 7a**. The robot's PS facilitates entry into the maxillary sinus through the ostium, while the spatial maneuverability of the DS covers most of the sinus cavity. Enhancing the robot's DOF in the frame is another effective method to increase flexibility. Kong et al.<sup>[270]</sup> developed an in situ torsionally steerable flexible robot, capable of rotating torsionally at constant positions and bending directions. This capability allows the robot to transmit torque for screwing actions in a bent state, as depicted in **Figure 7b**, and is particularly useful in laryngeal endoscopic surgery for maintaining the end-effector's position and approach vector throughout the procedure.

Furthermore, augmenting the stiffness of a continuum robot is crucial for improving operational precision. A common method to achieve this involves optimizing the robot's structural shape. Koszowska et al.<sup>[274]</sup> proposed a unique modular magnetic soft robot, composed of a soft magnetic double helix wrapped around a soft magnetic core. The seam of the double helix intersecting points provides planar reinforcement, significantly elevating bending stiffness along the XZ plane, as shown in **Figure 7c**. Li et al.<sup>[275]</sup> introduced an innovative metal printed continuum joint, integrating a variable pitch design into its springlike structure, effectively reducing positional errors at the joint's distal tip from 18.10% to 4.63%. Given the direct contact of continuous robots used in endoscopy with human soft tissues, research also concentrates on variable stiffness or rigid-flexible coupling features.<sup>[276]</sup> Luo et al.<sup>[48]</sup> devised a gastrointestinal endoscopic robot with a variable stiffness structure, whose stiffness adjustment mechanism is detailed in **Figure 7d**. This robot exhibits superior bending properties in both flexible and rigid states, consistent motion, and reliable shape-locking during rigid-flexible transitions, along with a high load-bearing capacity. Lastly, Li et al.<sup>[277]</sup> developed a novel teleoperated parallel continuum robot with adjustable stiffness, specifically for collision avoidance in transoral surgeries. The surgical outcomes indicate that this method can be preliminarily executed with success.

## 5.2. Actuation

Among the existing literatures surveyed, cable-driven actuation is the most common type for endoscopic surgery due to its

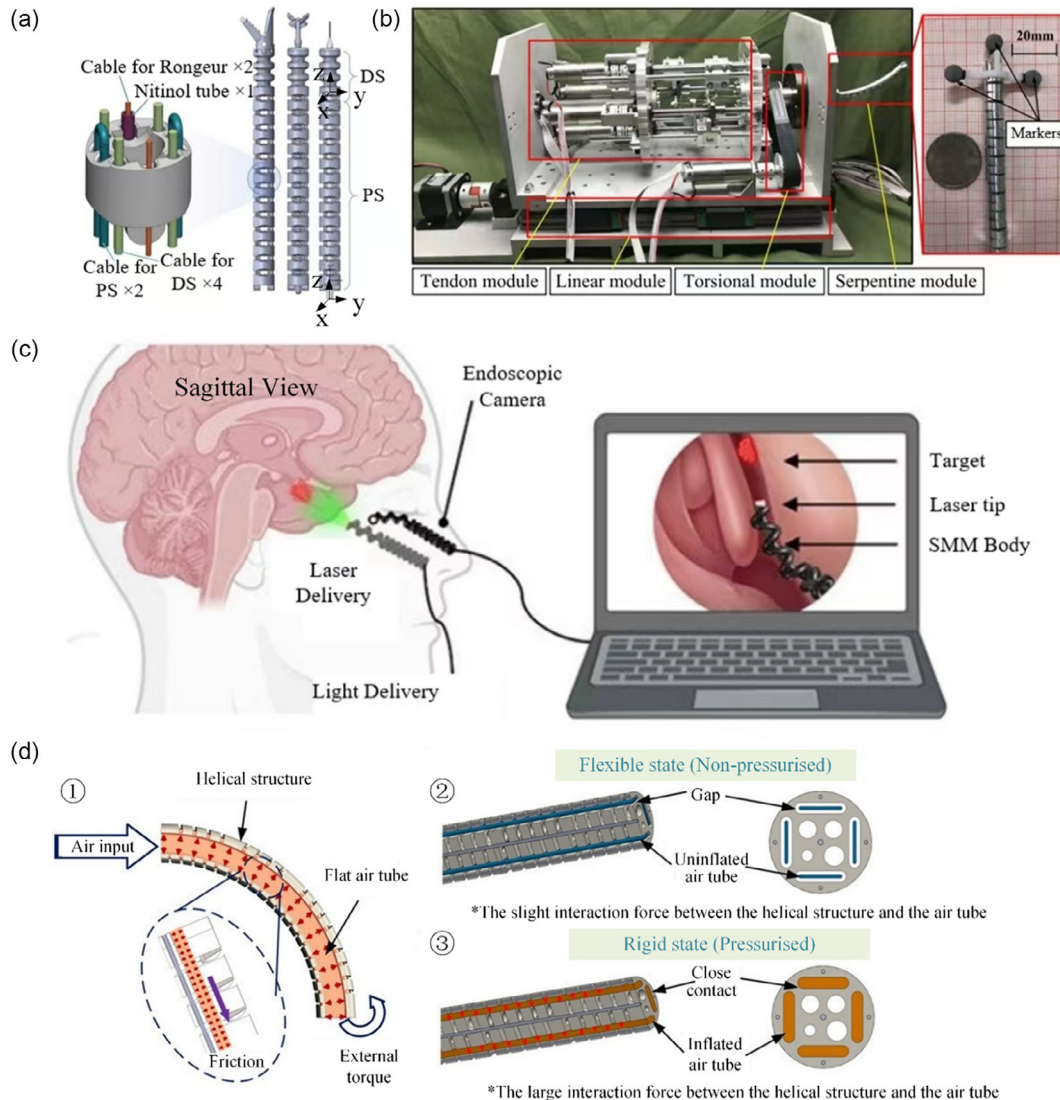


**Figure 7.** Illustration of advances in continuum robotics for endoscopic surgery: a) two-segment continuum modules with different functions. Reproduced with permission.<sup>[259]</sup> Copyright 2022, IEEE; b) a prototype of the in situ torsionally steerable robots for endoscopic surgery. Reproduced with permission.<sup>[270]</sup> Copyright 2022, IEEE; c) modular magnetic soft robot with high stiffness and its application. Reproduced with permission.<sup>[274]</sup> Copyright 2023, Wiley; and d) working principle illustration of the stiffness adjustment for gastrointestinal endoscopic robots. Reproduced with permission.<sup>[48]</sup> Copyright 2023, Wiley.

simplicity in design, ease of structural and performance expansion, low cost, and stability. However, due to its strong nonlinearity and inherent uncertainties, it leads to high dynamical uncertainties and low precision control. Garbin et al.<sup>[268,278]</sup> reported a fluid-driven endoscope continuum robot, but its driving characteristics result in a larger outer diameter, making it less suitable for surgical scenarios that require a microscale outer diameter. Campisano et al.<sup>[49–51]</sup> reported a robot based on water-jet actuation, which also resulted in a larger robot outer diameter for similar reasons as fluid-driven systems. Chautems et al. and Pittiglio et al.<sup>[53,54]</sup> used magnetic-driven actuation, a novel form of actuation that allows for simple design and smaller structural diameter but requires wireless control. However, this type of actuation requires more complex control logic

and can only achieve small actuation movements. Jacquemin et al.<sup>[279]</sup> introduced an innovative smart continuum actuator leveraging electroactive polymer, which exhibited remarkable performance, notably in bending capacity and control precision. Additionally, to improve the functionality of continuous robots, a combination of actuation methods has been employed. For instance, Wang et al.<sup>[273]</sup> combined hydraulic-driven mechanisms with tendons, enhancing the robot's agility in navigating to lesions and performing targeted laser sweeping on them. From a design trend perspective, cable-driven actuation will still be mainstream for microscale applications. Other actuation forms can be considered for larger scales or scenarios with lower requirements for interaction safety and motion control.



### 5.3. Sensing

In the realm of endoscopic surgery, vision-based sensors are predominantly utilized in robotic systems for functions like target-tracking feedback and robot self-pose control, as evidenced in studies.<sup>[54,280–282]</sup> Additionally, studies such as refs. [49–51,268,278,283,284] have implemented various sensors, including IMUs, gyroscopes, and EM-tracking-based devices, for shape-sensing purposes. Specifically, research of Gao et al.<sup>[284]</sup> has leveraged FBG sensors to monitor end strain, thereby facilitating force interaction with the environment. Moreover, advancements in sensing technology have led to the development of innovative components. For example, study of Yin et al.<sup>[285]</sup> introduced a novel miniature continuum surgical robot, characterized by a multi-material laminated structure. This design enables the integration of small piezoelectric transducers on the robot's surface, functioning as beacons to emit ultrasonic waves for the shape detection of the continuum robot. The performance of this technology demonstrated a less than 4 mm error in open-loop trajectory control without compensation, and less than 1 mm error in ultrasonic shape detection. However, these emerging sensors remain in the experimental stage and are not yet ready for clinical application. The future trend for endoscopic applications necessitates sensors that are compact, highly accurate in perception, flexible, and equipped with integrated multi-perception capabilities. Additionally, these hardware systems must undergo rigorous clinical testing and conform to medical device standards.

### 5.4. Control and Navigation

The control accuracy of endoscope continuum robots can be expressed in terms of end deviation/length. The existing robot control accuracy<sup>[49–51,280,281,283,286–289]</sup> is generally distributed between 1% and 10%. To harmonize control and navigation approaches with endoscopic surgical practices, the study predominantly focuses on simplifying control models and architectures. This simplification aims to facilitate multi-robot cooperation, improve the efficacy of motion planning, and foster adaptability in surgical contexts.

Simplification of control mechanisms is a critical aspect, as it can mitigate the difficulties experienced by surgeons during operations, thereby potentially increasing the success rates of these procedures. To reduce the computational complexity of control models, most research studies have used order-reduced modal models, such as PCC, CC, D–H, and other models.<sup>[53,54,249,268,272,278,290–293]</sup> However, research that utilizes models like the Cosserat rod model<sup>[49–51,284]</sup> achieves high computational complexity, resulting in lower control accuracy and real-time performance. With the emergence of learning-based methods, data-driven models, as used in refs. [282,284], may become future development trends. The combination of data-driven and model-based approaches also holds great potential. In the realm of structural complexity, scholars are focused on reducing reliance on sensors by improving control algorithms, a strategy that promises to streamline robot architecture. For example, prevalent research in active compliance and force sensing depends on force sensors located at either the proximal or

distal extremities of robots, which complicates the system. Wu et al.<sup>[294]</sup> introduced a novel approach, utilizing tip-pose feedback for active compliance and force estimation, thereby obviating the need for supplementary sensors apart from an endoscopic camera. In some scenarios, a single-continuum robot might prove insufficient for task completion, necessitating the orchestration of multiple such robots. This requires the autonomous operation of diverse robots in a limited area, with an emphasis on avoiding mutual interference. Koszowska et al.<sup>[274]</sup> developed methods for the autonomous magnetic operation of two magnetic continuum manipulators within the same constrained space. These manipulators maintain high autonomy and, when used in tandem, can effectively replicate the minimally invasive ablation of a pituitary adenoma.

In terms of motion planning, due to the need for endoscopic surgery in narrow and irregular environments, FTL is the mainstream motion planning method in current research.<sup>[54,283,292,293]</sup> Depending on the specific application requirements, three control patterns, autonomous,<sup>[54,249,282,283]</sup> master–slave,<sup>[268,278,290]</sup> and shared control,<sup>[49–51,280,281]</sup> have been applied. To improve motion planning efficiency in unstructured environments, Kuntz et al.<sup>[295]</sup> introduced a method that integrates sampling-based motion planning with local optimization. This approach effectively processes point cloud data and quickly generates high-quality plans. Its effectiveness was validated in three anatomical scenarios, including two based on endoscopic videos from actual patient anatomies. Considering the complex cavity structures in various organs, enhancing the adaptability of continuum robots remains a crucial research focus. To address this, Wang et al.<sup>[296]</sup> developed a hybrid adaptive control framework. This framework is designed to counteract uncertainties like friction, tendon relaxation in the driving mechanism, and external forces affecting the robot. This allows for rapid response and maintains a relatively high degree of positioning accuracy.

The existing research on endoscopes provides a crucial foundation for exploring continuum robots in arthroscopic procedures. This exploration not only encompasses the technologies integral to endoscopic continuum robots but also necessitates consideration of several additional aspects specific to arthroscopy.

### 5.5. Structural Miniaturization

The diameter of the lumen accommodating the endoscope is typically substantial. However, reducing the diameter of the arthroscope correlates with diminished tissue trauma during the procedure, which, in turn, accelerates patient recovery. Consequently, miniaturization is a crucial aspect in the development of arthroscopic continuum robots. This reduction in size also necessitates the integration of smaller and lighter sensors, including force and vision-based sensors.

### 5.6. High Motion Flexibility

The arthroscopic procedures require the ability to undergo large deformations within restricted spaces, which necessitates a high degree of motion flexibility. Particularly in cases where joint morphology is complex and the observational positioning is



constrained, arthroscopy necessitates the capacity for the robot to adjust its posture to facilitate effective observation.

### 5.7. High Stiffness

The miniaturization of the arthroscopic structure, while enhancing motion flexibility, could result in a reduction in its stiffness. This decrease may compromise the stability and operational precision required for surgical procedures. Consequently, it is imperative to advance stiffness technology for small-scale structures susceptible to significant deformations. Enhancing this aspect will improve the functional performance of continuous robots employed in arthroscopic surgeries, ensuring that they meet the rigorous demands of such medical interventions.

The employment of continuum robots in endoscopy has been the subject of considerable theoretical and experimental investigation, yet their implementation in large-scale clinical trials remains unexecuted. The exploration of continuum robots within the realm of arthroscopy is still in its nascent stages. For the effective integration of continuum robots in arthroscopic procedures, it is imperative to address not only the previously mentioned technological challenges but also to focus on the standardization, universality, and enhanced reliability of these robotic systems. A high degree of integration with surgical protocols is essential to fulfill the specific demands of arthroscopic surgery.

## 6. Conclusion

There have been numerous reports on continuum robots in the past few years.<sup>[29,55,75,107,108,188,250,297–299]</sup> These reports provide detailed discussions on the actuation, structure, sensing, and control of continuum robots. However, unlike previous reviews, this article focuses primarily on the requirements of arthroscopic continuum robots. It analysed the advantages and disadvantages of existing technologies in terms of motion, structure, sensing, and control. Additionally, by reviewing the literature on endoscopic continuum robots over the past decade, it presents the characteristics, limitations, and future development trends of various technologies. Due to the demand for arthroscopic surgery and the barriers posed by current continuum robot technologies, there is currently no mature solution for arthroscopic continuum robots that have a small diameter, high flexibility, and advanced navigation capabilities. It is crucial to address the design issues of small-diameter structures by considering their structure and materials. Similarly, high-precision control problems of small-diameter continuum robots can be resolved through intelligent sensing. Furthermore, intelligent navigation of robots and ensuring human–robot interaction safety can be achieved by developing optimization kinematic and dynamic models, as well as compliant control methods based on the assumption of constant curvature.

## Acknowledgements

This research was funded by National Natural Science Foundation of China (no. 31872310) and the Key Research and Development Program of Shandong Province (no. 2021SFGC0502).

## Conflict of Interest

The authors declare no conflict of interest.

## Keywords

arthroscopic surgery, bionics, continuum robotics, control, endoscope, structure design

Received: September 28, 2023

Revised: December 3, 2023

Published online:

- [1] A. Deodhar, J. H. Stone, in *A Clinician's Pearls & Myths in Rheumatology* (Ed: J. H. Stone), Springer International Publishing, Cham **2023**, pp. 621–634.
- [2] D. Kesharwani, S. Das Paul, R. Paliwal, T. Satapathy, *Colloids Surf., B* **2023**, *223*, 113160.
- [3] J. W.-P. Michael, K. U. Schlüter-Brust, P. Eysel, *Dtsch. Arztebl. Int.* **2010**, *107*, 152.
- [4] J. Y. Lee, Z. Y. Chia, L. Jiang, B. Ang, P. Chang, *Arthrosc. Tech.* **2020**, *9*, e435.
- [5] A. Badia, *J. Hand Surg., Am. Vol.* **2007**, *32A*, 707.
- [6] C. L. Baker, A. A. Brooks, *Clin. Sports Med.* **1996**, *15*, 261.
- [7] T. Matsuura, H. Egawa, M. Takahashi, K. Higashino, T. Sakai, N. Suzue, D. Hamada, T. Goto, Y. Takata, T. Nishisho, Y. Goda, *J. Med. Invest.* **2014**, *61*, 233.
- [8] G. I. Bain, A. Baker, T. L. Whipple, G. G. Poehling, C. Mathoulin, P.-C. Ho, *J. Wrist Surg.* **2022**, *11*, 96.
- [9] T. Pillukat, M. Muhldorfer-Fodor, J. Windolf, J. van Schoonhoven, *Orthopade* **2018**, *47*, 647.
- [10] J. Vega, M. Dalmau-Pastor, F. Malagelada, B. Fargues-Polo, F. Pena, *J. Bone Jt. Surg., Am. Vol.* **2017**, *99*, 1395.
- [11] J. C. Cheng, R. D. Ferkel, *Clin. Orthop. Relat. Res.* **1998**, *349*, 65.
- [12] A. O. Elmlund, I. G. Winson, *Foot Ankle Clin.* **2015**, *20*, 71.
- [13] J. I. Acevedo, R. C. Palmer, P. G. Mangone, *Foot Ankle Clin.* **2018**, *23*, 555.
- [14] J. E. Adams, S. P. Steinmann, R. W. Culp, *Hand Clin.* **2011**, *27*, 355.
- [15] X. Zhang, T. Wang, S. Wan, *J. Hand Surg., Am. Vol.* **2015**, *40*, 152.
- [16] V. D. Shetty, R. N. Villar, *Br. J. Sports Med.* **2007**, *41*, 64.
- [17] A. C. L. Magrill, N. Nakano, V. Khanduja, *Int. Orthop.* **2017**, *41*, 1983.
- [18] A. Boese, C. Wex, R. Croner, U. B. Liehr, J. J. Wendler, J. Weigt, T. Walles, U. Vorwerk, C. H. Lohmann, M. Friebe, A. Illanes, *Diagnostics* **2022**, *12*, 1262.
- [19] L. Wu, A. Jaiprakash, A. K. Pandey, D. Fontanarosa, Y. Jonmohamadi, M. Antico, M. Strydom, A. Razjigaev, F. Sasazawa, J. Roberts, R. Crawford, in *29 -Robotic and Image-Guided Knee Arthroscopy* (Eds: M.H.B.T.-H. of R., I.-G. S. Abedin-Nasab), Elsevier, Amsterdam, Netherlands **2020**, pp. 493–514.
- [20] A. J. Price, G. Erturan, K. Akhtar, A. Judge, A. Alvand, J. L. Rees, *Bone Joint J.* **2015**, *97*, 1309.
- [21] R. J. Webster, III, B. A. Jones, *Int. J. Rob. Res.* **2010**, *29*, 1661.
- [22] G. Robinson, J. B. C. Davies, in *Proc. 1999 IEEE Int. Conf. Robotics and Automation (Cat. No. 99CH36288C)*, IEEE, Piscataway, NJ **1999**, pp. 2849–2854.
- [23] B. A. Jones, I. D. Walker, *IEEE Trans. Rob.* **2006**, *22*, 1087.
- [24] J. Burgner-Kahrs, D. C. Rucker, H. Choset, *IEEE Trans. Rob.* **2015**, *31*, 1261.
- [25] K. H. Lee, K. C. D. Fu, Z. Guo, Z. Dong, M. C. Leong, C. L. Cheung, A. P. W. Lee, W. Luk, K. W. Kwok, *IEEE/ASME Trans. Mechatron.* **2018**, *23*, 586.

- [26] X. Wang, K. H. Lee, D. K. Fu, Z. Dong, K. Wang, G. Fang, S. L. Lee, A. P. Lee, K. W. Kwok, *Int. J. Comput. Assisted Radiol. Surg.* **2018**, *13*, 797.
- [27] F. Iida, C. Laschi, *Procedia Comput. Sci.* **2011**, *7*, 99.
- [28] D. Trivedi, C. D. Rahn, W. M. Kier, I. D. Walker, *Appl. Bionics Biomech.* **2008**, *5*, 99.
- [29] I. A. Seleem, H. El-Hussieny, H. Ishii, *Int. J. Control Autom. Syst.* **2023**, *21*, 1592.
- [30] Z. Li, R. Du, *Int. J. Adv. Rob. Syst.* **2013**, *10*, 209.
- [31] D. M. Aukes, B. Heyneman, J. Ulmen, H. Stuart, M. R. Cutkosky, S. Kim, P. Garcia, A. Edsinger, *Int. J. Rob. Res.* **2014**, *33*, 721.
- [32] M. Manti, T. Hassan, G. Passetti, N. D'Elia, C. Laschi, M. Cianchetti, *Soft Rob.* **2015**, *2*, 107.
- [33] W. McMahan, B. A. Jones, I. D. Walker, in *2005 IEEE/RSJ Int. Conf. Intelligent Robots and Systems*, IEEE, Piscataway, NJ **2005**, pp. 2578–2585.
- [34] R. K. Katzschmann, A. D. Marchese, D. Rus, in *Experimental Robotics*, Springer, Berlin, Heidelberg **2016**, pp. 405–420.
- [35] T. TolleyMichael, F. ShepherdRobert, C. GallowayKevin, J. WoodRobert, M. WhitesidesGeorge, *Soft Rob.* **2014**, *1*, 213.
- [36] N. W. Bartlett, M. T. Tolley, J. T. Overvelde, J. C. Weaver, B. Mosadegh, K. Bertoldi, G. M. Whitesides, R. J. Wood, *Science* **2015**, *349*, 161.
- [37] C. D. Onal, X. Chen, G. M. Whitesides, D. Rus, in *Robotics Research*, Springer, Berlin, Heidelberg **2017**, pp. 525–540.
- [38] T. Umedachi, V. Vikas, B. A. Trimmer, *Bioinspiration Biomimetics* **2016**, *11*, 25001.
- [39] A. Villoslada, A. Flores, D. Copaci, D. Blanco, L. Moreno, *Rob. Auton. Syst.* **2015**, *73*, 91.
- [40] S. Shian, K. Bertoldi, D. R. Clarke, *Adv. Mater.* **2015**, *27*, 6814.
- [41] I. A. Anderson, T. A. Gisby, T. G. McKay, B. M. O'Brien, E. P. Calius, *J. Appl. Phys.* **2012**, *112*, 41101.
- [42] P. Chakraborti, H. A. K. Toprakci, P. Yang, N. Di Spigna, P. Franzon, T. Ghosh, *Sens. Actuators, A* **2012**, *179*, 151.
- [43] S. Koshima, F. Miyasaka, K. Hirata, *IEEE Trans. Magn.* **2012**, *48*, 1649.
- [44] C. Guo, C. Wu, H. Liu, *J. Mech. Eng.* **2017**, *53*, 1.
- [45] Y. Huang, Y. Xu, H. K. Bisoyi, Z. Liu, J. Wang, Y. Tao, T. Yang, S. Huang, H. Yang, Q. Li, *Adv. Mater.* **2023**, *35*, 2304378.
- [46] J. Gao, Y. Tang, D. Martella, J. Guo, D. S. Wiersma, Q. Li, *Responsive Mater.* **2023**, *1*, e20230008.
- [47] Y. Wang, A. Dang, Z. Zhang, R. Yin, Y. Gao, L. Feng, S. Yang, *Adv. Mater.* **2020**, *32*, 2004270.
- [48] X. Luo, D. Song, Z. Zhang, S. Wang, C. Shi, *Adv. Intell. Syst.* **2023**, *5*, 2200403.
- [49] F. Campisano, A. A. Ramirez, C. A. Landewee, S. Caló, K. L. Obstein, R. J. Webster, P. Valdastrì, *IEEE Rob. Autom. Lett.* **2020**, *5*, 6427.
- [50] F. Campisano, A. A. Ramirez, S. Caló, J. H. Chandler, K. L. Obstein, R. J. Webster, P. Valdastrì, *IEEE Rob. Autom. Lett.* **2020**, *5*, 2642.
- [51] F. Campisano, F. Gramuglia, I. R. Dawson, C. T. Lyne, M. L. Izmaylov, S. Misra, E. De Momi, D. R. Morgan, K. L. Obstein, P. Valdastrì, *IEEE Rob. Autom. Mag.* **2017**, *24*, 73.
- [52] T. Zhang, L. Yang, X. Yang, R. Tan, H. Lu, Y. Shen, *Adv. Intell. Syst.* **2021**, *3*, 2000189.
- [53] C. Chautems, A. Tonazzini, Q. Boehler, S. H. Jeong, D. Floreano, B. J. Nelson, *Adv. Intell. Syst.* **2020**, *2*, 1900086.
- [54] G. Pittiglio, P. Lloyd, T. da Veiga, O. Onaizah, C. Pompili, J. H. Chandler, P. Valdastrì, *Soft Rob.* **2022**, *9*, 1120.
- [55] J. Wang, A. Chortos, *Adv. Intell. Syst.* **2022**, *4*, 2100165.
- [56] X. Chen, X. Zhang, Y. Huang, L. Cao, J. Liu, *J. Field Rob.* **2022**, *39*, 281.
- [57] F. Xu, H. Wang, *IEEE-CAA J. Autom. Sin.* **2021**, *8*, 1500.
- [58] W. Dou, G. Zhong, J. Cao, Z. Shi, B. Peng, L. Jiang, *Adv. Mater. Technol.* **2021**, *6*, 2100018.
- [59] T. da Veiga, J. H. Chandler, P. Lloyd, G. Pittiglio, N. J. Wilkinson, A. K. Hoshiar, P. Valdastrì, *Prog. Biomed. Eng.* **2020**, *2*, 32003.
- [60] A. L. Orekhov, C. Abah, N. Simaan, *The Encyclopedia of Medical Robotics*, World Scientific, Singapore **2018**, pp. 203–243.
- [61] J. P. Swensen, M. D. Lin, A. M. Okamura, N. J. Cowan, *IEEE Trans. Biomed. Eng.* **2014**, *61*, 2707.
- [62] A. Favaro, R. Secoli, F. R. Y. Baena, E. De Momi, *IEEE Rob. Autom. Lett.* **2020**, *5*, 6780.
- [63] P. J. Swaney, J. Burgner, H. B. Gilbert, R. J. Webster, *IEEE Trans. Biomed. Eng.* **2012**, *60*, 906.
- [64] P. E. Dupont, J. Lock, B. Itkowitz, E. Butler, *IEEE Trans. Rob.* **2009**, *26*, 209.
- [65] D. C. Rucker, R. J. Webster, G. S. Chirikjian, N. J. Cowan, *Int. J. Rob. Res.* **2010**, *29*, 1263.
- [66] Z. Li, L. Wu, H. Ren, H. Yu, *Mech. Mach. Theory* **2017**, *107*, 148.
- [67] Q. Peyron, K. Rabenoroosa, N. Andreff, P. Renaud, *Mech. Mach. Theory* **2019**, *132*, 176.
- [68] T. Liu, G. Zhang, P. Zhang, T. Cheng, Z. Luo, S. Wang, F. Du, *Sensors* **2023**, *23*, 3709.
- [69] Y. Chitalia, N. J. Deaton, S. Jeong, N. Rahman, J. P. Desai, *IEEE Rob. Autom. Lett.* **2020**, *5*, 1712.
- [70] W. Zeng, J. Yan, K. Yan, X. Huang, X. Wang, S. S. Cheng, *IEEE Rob. Autom. Lett.* **2021**, *6*, 6489.
- [71] J. Liu, S. Shang, G. Zhang, S. Xue, H. Cheng, P. Qi, F. Du, *Machines* **2022**, *10*, 778.
- [72] P. Berthet-Rayne, G. Gras, K. Leibrandt, P. Wisanuvej, A. Schmitz, C. A. Seneci, G. Z. Yang, *Ann. Biomed. Eng.* **2018**, *46*, 1663.
- [73] A. Yeshmukhametov, K. Koganezawa, Y. Yamamoto, Z. Buribayev, Z. Mukhtar, Y. Amirgaliyev, *Appl. Sci.* **2022**, *12*, 6922.
- [74] N. Simaan, K. Xu, W. Wei, A. Kapoor, P. Kazanzides, R. Taylor, P. Flint, *Int. J. Rob. Res.* **2009**, *28*, 1134.
- [75] T. Kato, I. Okumura, H. Kose, K. Takagi, N. Hata, *Int. J. Comput. Assisted Radiol. Surg.* **2016**, *11*, 589.
- [76] K. B. Reed, A. Majewicz, V. Kallem, R. Alterovitz, K. Goldberg, N. J. Cowan, A. M. Okamura, *IEEE Rob. Autom. Mag.* **2011**, *18*, 35.
- [77] D. S. Minhas, J. A. Engh, M. M. Fenske, C. N. Riviere, in *2007 29th Annual Int. Conf. IEEE Engineering in Medicine and Biology Society*, IEEE, Piscataway, NJ **2007**, pp. 2756–2759.
- [78] S. Okazawa, R. Ebrahimi, J. Chuang, S. E. Salcudean, R. Rohling, *IEEE/ASME Trans. Mechatron.* **2005**, *10*, 285.
- [79] M. Khadem, C. Rossa, N. Usmani, R. S. Sloboda, M. Tavakoli, *IEEE J. Biomed. Health Inform.* **2017**, *22*, 1917.
- [80] R. J. Roesthuis, N. J. van de Berg, J. J. van den Dobbelen, S. Misra, in *2015 IEEE Int. Conf. Robotics and Automation (ICRA)*, IEEE, Piscataway, NJ **2015**, pp. 2283–2289.
- [81] A. Hong, Q. Boehler, R. Moser, A. Zemmar, L. Stieglitz, B. J. Nelson, *Int. J. Med. Rob. Comput. Assisted Surg.* **2019**, *15*, e1998.
- [82] P. Sears, P. Dupont, in *2006 IEEE/RSJ Int. Conf. Intelligent Robots and Systems*, IEEE, Piscataway, NJ **2006**, pp. 2850–2856.
- [83] H. B. Gilbert, D. C. Rucker, R. J. Webster, III, in *Robotics Research: The 16th Int. Symp. ISRR*, Springer, Berlin, Heidelberg **2016**, pp. 253–269.
- [84] C. R. Mitchell, R. J. Hendrick, R. J. Webster, III, S. D. Herrell, *J. Endourol.* **2016**, *30*, 692.
- [85] S. Amack, M. Rox, J. Mitchell, T. E. Ertop, M. Emerson, A. Kuntz, J. Mitchell, T. E. Ertop, J. Gafford, F. Maldonado, J. Akulian, in *Medical Imaging 2019: Image-Guided Procedures, Robotic Interventions, and Modeling*, SPIE, Bellingham, WA, USA **2019**, pp. 114–121.
- [86] J. B. Gafford, S. Webster, N. Dillon, E. Blum, R. Hendrick, F. Maldonado, E. A. Gillaspie, O. B. Rickman, S. Duke Herrell, R. J. Webster, *Ann. Biomed. Eng.* **2020**, *48*, 181.
- [87] K. E. Riojas, R. J. Hendrick, R. J. Webster, *IEEE Rob. Autom. Lett.* **2018**, *3*, 1624.

- [88] E. Amanov, T.-D. Nguyen, J. Burgner-Kahrs, *Int. J. Rob. Res.* **2021**, *40*, 7.
- [89] M. S. Moses, R. J. Murphy, M. D. M. Kutzer, M. Armand, *IEEE/ASME Trans. Mechatron.* **2015**, *20*, 2876.
- [90] S. Yoshida, T. Kanno, K. Kawashima, *J. Mech. Rob.* **2018**, *10*, 31011.
- [91] R. J. Murphy, M. D. M. Kutzer, S. M. Segreti, B. C. Lucas, M. Armand, *Robotica* **2014**, *32*, 835.
- [92] P. Francis, K. W. Eastwood, V. Bodani, K. Price, K. Upadhyaya, D. Podolsky, H. Azimian, T. Looi, J. Drake, *IEEE Rob. Autom. Mag.* **2017**, *24*, 24.
- [93] Y. Y. Zhou, J. H. Li, M. Q. Guo, Z. D. Wang, H. Liu, *Robot* **2020**, *42*, 316.
- [94] D. C. Rucker, R. J. Webster, III, *IEEE Trans. Rob.* **2011**, *27*, 1033.
- [95] K. Oliver-Butler, J. Till, C. Rucker, *IEEE Trans. Rob.* **2019**, *35*, 403.
- [96] T.-D. Nguyen, J. Burgner-Kahrs, in *2015 IEEE/RSJ Int. Conf. Intelligent Robots and Systems (IROS)*, IEEE, Piscataway, NJ **2015**, pp. 2130–2135.
- [97] B. Kang, R. Kojcev, E. Sinibaldi, *PLoS One* **2016**, *11*, 0150278.
- [98] D.-G. Choi, B.-J. Yi, W.-K. Kim, in *2007 IEEE/RSJ Int. Conf. Intelligent Robots and Systems*, IEEE, Piscataway, NJ **2007**, pp. 1815–1821.
- [99] Y. Kim, S. S. Cheng, J. P. Desai, *IEEE Trans. Rob.* **2017**, *34*, 18.
- [100] A. Ataollahi, R. Karim, A. S. Fallah, K. Rhode, R. Razavi, L. D. Seneviratne, T. Schaeffter, K. Althoefer, *IEEE Trans. Biomed. Eng.* **2013**, *63*, 2425.
- [101] J. Tian, T. Wang, X. Fang, Z. Shi, *Smart Mater. Struct.* **2020**, *29*, 045007.
- [102] F. Maghooa, A. Stilli, Y. Noh, K. Althoefer, H. A. Wurdemann, in *2015 IEEE Int. Conf. Robotics and Automation (ICRA)*, IEEE, Piscataway, NJ **2015**, pp. 2556–2561.
- [103] J.-Y. Lee, E.-Y. Go, W.-Y. Choi, W.-B. Kim, K.-J. Cho, in *2016 13th Int. Conf. Ubiquitous Robots and Ambient Intelligence (URAI)*, IEEE, Piscataway, NJ **2016**, pp. 377–379.
- [104] Y.-J. Kim, S. Cheng, S. Kim, K. Iagnemma, *IEEE Trans. Rob.* **2013**, *29*, 1031.
- [105] D. C. F. Li, Z. Wang, B. Ouyang, Y.-H. Liu, in *2019 Int. Conf. Robotics and Automation (ICRA)*, IEEE, Piscataway, NJ **2019**, pp. 3976–3982.
- [106] Z. Li, J. Feiling, H. Ren, H. Yu, *Engineering* **2015**, *1*, 73.
- [107] C. Shi, X. Luo, P. Qi, T. Li, S. Song, Z. Najdovski, T. Fukuda, H. Ren, *IEEE Trans. Biomed. Eng.* **2017**, *64*, 1665.
- [108] A. A. Nazari, K. Zareinia, F. Janabi-Sharifi, *Int. J. Med. Rob. Comput. Assisted Surg.* **2022**, *18*, e2384.
- [109] G. Gerboni, A. Diodato, G. Ciuti, M. Cianchetti, A. Menciassi, *IEEE/ASME Trans. Mechatron.* **2017**, *22*, 1881.
- [110] J. T. Muth, D. M. Vogt, R. L. Truby, Y. Mengüç, D. B. Kolesky, R. J. Wood, J. A. Lewis, *Adv. Mater.* **2014**, *26*, 6307.
- [111] Z. Shi, J. Tian, R. Luo, G. Zhao, T. Wang, *IEEE Trans. Syst. Man Cybern. Syst.* **2017**, *48*, 1106.
- [112] S. C. B. Mannsfeld, B. C. K. Tee, R. M. Stoltenberg, C. V. Chen, S. Barman, B. V. O. Muir, A. N. Sokolov, C. Reese, Z. Bao, *Nat. Mater.* **2010**, *9*, 859.
- [113] Q. Shen, T. Wang, K. J. Kim, *Bioinspiration Biomimetics* **2015**, *10*, 55007.
- [114] R. K. Kramer, C. Majidi, R. J. Wood, in *2011 IEEE Int. Conf. Robotics and Automation*, IEEE, Piscataway, NJ **2011**, pp. 1103–1107.
- [115] R. K. Kramer, C. Majidi, R. J. Wood, *Adv. Funct. Mater.* **2013**, *23*, 5292.
- [116] Y.-L. Park, B.-R. Chen, R. J. Wood, *IEEE Sens. J.* **2012**, *12*, 2711.
- [117] R. A. Bilodeau, E. L. White, R. K. Kramer, in *2015 IEEE/RSJ Int. Conf. Intelligent Robots and Systems (IROS)*, IEEE, Piscataway, NJ **2015**, pp. 2324–2329.
- [118] S. Sareh, A. Jiang, A. Faragasso, Y. Noh, T. Nanayakkara, P. Dasgupta, L. D. Seneviratne, H. A. Wurdemann, K. Althoefer, in *2014 IEEE Int. Conf. Robotics and Automation*, IEEE, Piscataway, NJ **2014**, pp. 1454–1459.
- [119] T. C. Searle, K. Althoefer, L. Seneviratne, H. Liu, in *2013 IEEE Int. Conf. Robotics and Automation*, IEEE, Piscataway, NJ **2013**, pp. 4415–4420.
- [120] S. Sareh, Y. Noh, M. Li, T. Ranzani, H. Liu, K. Althoefer, *Smart Mater. Struct.* **2015**, *24*, 125024.
- [121] Y.-L. Park, S. Elayaperumal, B. Daniel, S. C. Ryu, M. Shin, J. Savall, R. J. Black, B. Moslehi, M. R. Cutkosky, *IEEE/ASME Trans. Mechatron.* **2010**, *15*, 906.
- [122] S. Elayaperumal, J. C. Plata, A. B. Holbrook, Y. L. Park, K. B. Pauly, B. L. Daniel, M. R. Cutkosky, *IEEE Trans. Med. Imaging* **2014**, *33*, 2128.
- [123] R. J. Roesthuis, M. Kemp, J. J. van den Dobbelsteen, S. Misra, *IEEE/ASME Trans. Mechatron.* **2014**, *19*, 1115.
- [124] R. J. Roesthuis, S. Misra, *IEEE Trans. Rob.* **2016**, *32*, 372.
- [125] H. Liu, A. Farvadin, S. A. Pedram, I. Iordachita, R. H. Taylor, M. Armand, in *2015 IEEE Int. Conf. Robotics and Automation (ICRA)*, IEEE, Piscataway, NJ **2015**, pp. 201–206.
- [126] H. Liu, A. Farvadin, R. Grupp, R. J. Murphy, R. H. Taylor, I. Iordachita, M. Armand, *IEEE Sens. J.* **2015**, *15*, 5494.
- [127] L. W. Zhang, J. W. Qian, L. Y. Shen, Y. N. Zhang, in *2004 IEEE Int. Conf. Robotics and Automation, Volume 1–5, Proc.*, IEEE, Piscataway, NJ **2004**, pp. 835–840.
- [128] J. C. Yi, X. J. Zhu, L. Y. Shen, B. Sun, L. N. Jiang, in *Int. Conf. Life System Modeling and Simulation/Int. Conf. Intelligent Computing for Sustainable Energy and Environment (LSMS-ICSEE)*, Springer, Berlin, Heidelberg **2010**, pp. 25–31.
- [129] K. R. Henken, J. Dankelman, J. J. van den Dobbelsteen, L. K. Cheng, M. S. van der Heiden, *IEEE/ASME Trans. Mechatron.* **2014**, *19*, 1523.
- [130] C. Ledermann, H. Pauer, O. Weede, H. Woern, in *Proc. 2013 6th IEEE Conf. Robotics, Automation and Mechatronics (RAM)*, IEEE, Piscataway, NJ **2013**, pp. 195–200.
- [131] N. J. Deaton, M. Sheft, J. P. Desai, *IEEE/ASME Trans. Mechatron.* **2023**, *28*, 3041.
- [132] S. Sefati, R. Hegeman, F. Alambeigi, I. Iordachita, P. Kazanzides, H. Khanuja, R. H. Taylor, M. Armand, *IEEE/ASME Trans. Mechatron.* **2021**, *26*, 369.
- [133] P. Polygerinos, D. Zbyszewski, T. Schaeffter, R. Razavi, L. D. Seneviratne, K. Althoefer, *IEEE Sens. J.* **2010**, *10*, 1598.
- [134] F. Taffoni, D. Formica, P. Saccomandi, G. Di Pino, E. Schena, *Sensors* **2013**, *13*, 14105.
- [135] A. A. G. Abushagur, N. Arsad, M. I. Reaz, A. A. A. Bakar, *Sensors* **2014**, *14*, 6633.
- [136] Y. Sun, S. Song, X. Liang, H. Ren, *IEEE Rob. Autom. Lett.* **2016**, *1*, 617.
- [137] A. M. Franz, T. Haidegger, W. Birkfellner, K. Cleary, T. M. Peters, L. Maier-Hein, *IEEE Trans. Med. Imaging* **2014**, *33*, 1702.
- [138] X. B. Luo, Y. Wan, X. J. He, K. Mori, *Med. Image Anal.* **2015**, *24*, 282.
- [139] C. Y. Shi, C. Tercero, S. Ikeda, T. Fukuda, K. Komori, K. Yamamoto, in *2011 IEEE/RSJ Int. Conf. Intelligent Robots and Systems*, IEEE, Piscataway, NJ **2011**.
- [140] C. Y. Shi, C. Tercero, X. L. Wu, S. Ikeda, K. Komori, K. Yamamoto, F. Arai, T. Fukuda, *Int. J. Med. Rob. Comput. Assisted Surg.* **2016**, *12*, 648.
- [141] C. A. Linte, J. White, R. Eagleson, G. M. Guiraudon, T. M. Peters, *IEEE Rev. Biomed. Eng.* **2010**, *3*, 25.
- [142] Y. Ganji, F. Janabi-Sharifi, A. N. Cheema, *Int. J. Comput. Assisted Radiol. Surg.* **2009**, *4*, 307.
- [143] A. P. Shah, P. A. Kupelian, T. R. Willoughby, S. L. Meeks, *J. Appl. Clin. Med. Phys.* **2011**, *12*, 34.
- [144] E. Lugez, H. Sadjadi, D. R. Pichora, R. E. Ellis, S. G. Akl, G. Fichtinger, *Int. J. Comput. Assisted Radiol. Surg.* **2015**, *10*, 253.



- [145] H. Sadjadi, K. Hashtrudi-Zaad, G. Fichtinger, *Int. J. Med. Rob. Comput. Assisted Surg.* **2016**, 12, 189.
- [146] T. Reichl, J. Gardiazabal, N. Navab, *IEEE Trans. Med. Imaging* **2013**, 32, 1526.
- [147] X. B. Luo, Y. Wan, X. J. He, *Med. Phys.* **2015**, 42, 1808.
- [148] X. B. Luo, M. Feuerstein, D. Deguchi, T. Kitasaka, H. Takabatake, K. Mori, *Med. Image Anal.* **2012**, 16, 577.
- [149] M. Nakamoto, K. Nakada, Y. Sato, K. Konishi, M. Hashizume, S. Tamura, *IEEE Trans. Med. Imaging* **2008**, 27, 255.
- [150] M. Feuerstein, T. Reichl, J. Vogel, J. Traub, N. Navab, *IEEE Trans. Med. Imaging* **2009**, 28, 951.
- [151] S. Song, Z. Li, M. Q.-H. Meng, H. Yu, H. Ren, *IEEE Sens. J.* **2015**, 15, 6326.
- [152] J. Huang, W. G. Huo, W. X. Xu, S. Mohammed, Y. Amirat, *IEEE Trans. Autom. Sci. Eng.* **2015**, 12, 1257.
- [153] Y. L. Fu, H. Liu, S. G. Wang, W. Deng, X. L. Li, Z. G. Liang, *Int. J. Med. Rob. Comput. Assisted Surg.* **2009**, 5, 125.
- [154] S. Condino, E. M. Calabro, A. Alberti, S. Parrini, R. Cioni, R. N. Berchiolli, M. Gesi, V. Ferrari, M. Ferrari, *Eur. J. Vasc. Endovasc. Surg.* **2014**, 47, 53.
- [155] H. Sadjadi, K. Hashtrudi-Zaad, G. Fichtinger, *IEEE Trans. Biomed. Eng.* **2016**, 63, 1771.
- [156] S. Tully, G. Kantor, M. A. Zenati, H. Choset, in *2011 IEEE/RSJ Int. Conf. Intelligent Robots and Systems*, IEEE, Piscataway, NJ **2011**, pp. 1353–1358.
- [157] S. Tully, H. Choset, *IEEE Trans. Biomed. Eng.* **2016**, 63, 392.
- [158] S. Song, Z. Li, H. Y. Yu, H. L. Ren, *IEEE Sens. J.* **2015**, 15, 4565.
- [159] L. Wu, S. Song, K. Y. Wu, C. M. Lim, H. L. Ren, *Med. Biol. Eng. Comput.* **2017**, 55, 403.
- [160] A. Dore, G. Smoljic, E. V. Poorten, M. Sette, J. V. Sloten, G. Z. Yang, in *2012 IEEE/RSJ Int. Conf. Intelligent Robots and Systems (IROS)*, IEEE, Piscataway, NJ **2012**, pp. 3806–3811.
- [161] V. K. Chitrakaran, A. Behal, D. M. Dawson, I. D. Walker, *Robotica* **2007**, 25, 581.
- [162] J. M. Croom, D. C. Rucker, J. M. Romano, R. J. Webster, in *2010 IEEE Int. Conf. Robotics And Automation (ICRA)*, IEEE, Piscataway, NJ **2010**, pp. 4591–4596.
- [163] B. Weber, P. Zeller, K. Kuhnlenz, in *2012 IEEE/RSJ Int. Conf. Intelligent Robots and Systems (IROS)*, IEEE, Piscataway, NJ **2012**, pp. 3350–3355.
- [164] W. J. Xu, R. P. L. Foong, H. L. Ren, in *2015 IEEE Int. Conf. Information and Automation*, IEEE, Piscataway, NJ **2015**, pp. 637–642.
- [165] C. Papalazarou, P. M. J. Rongen, P. H. N. de With, in *Medical Imaging 2012: Image-Guided Procedures, Robotic Interventions, and Modeling*, Vol. 8316, SPIE, Bellingham, WA, USA **2012**.
- [166] M. Wagner, S. Schafer, C. Strother, C. Mistretta, *Med. Phys.* **2016**, 43, 1324.
- [167] M. Hoffmann, A. Brost, M. Koch, F. Bourier, A. Maier, K. Kurzdin, N. Strobel, J. Hornegger, *IEEE Trans. Med. Imaging* **2016**, 35, 567.
- [168] E. J. Lobaton, J. H. Fu, L. G. Torres, R. Alterovitz, in *2013 IEEE Int. Conf. Robotics And Automation (ICRA)*, IEEE, Piscataway, NJ **2013**, pp. 725–732.
- [169] Y. Otake, R. J. Murphy, M. D. Kutzer, R. H. Taylor, M. Armand, in *Medical Imaging 2014: Image-Guided Procedures, Robotic Interventions, and Modeling*, Vol. 9036, SPIE, Bellingham, WA, USA **2014**.
- [170] P. Mountney, D. Stoyanov, G. Z. Yang, *IEEE Signal Process. Mag.* **2010**, 27, 14.
- [171] X. B. Luo, A. J. McLeod, U. L. Jayarathne, S. E. Pautler, C. M. Schlachta, T. M. Peters, in *Medical Imaging 2016: Image-Guided Procedures, Robotic Interventions, and Modeling*, Vol. 9786, SPIE, Bellingham, WA, USA **2016**.
- [172] B. X. Lin, Y. Sun, X. N. Qian, D. Goldgof, R. Gitlin, Y. C. You, *Int. J. Med. Rob. Comput. Assisted Surg.* **2016**, 12, 158.
- [173] L. Maier-Hein, P. Mountney, A. Bartoli, H. Elhawary, D. Elson, A. Groch, A. Kolb, M. Rodrigues, J. Sorger, S. Speidel, D. Stoyanov, *Med. Image Anal.* **2013**, 17, 974.
- [174] X. Luo, U. L. Jayarathne, S. E. Pautler, T. M. Peters, in *Image and Graphics* (Ed: Y.-J. Zhang), Springer International Publishing, Cham **2015**, pp. 664–676.
- [175] R. Reilink, S. Stramigioli, S. Misra, *Int. J. Comput. Assisted Radiol. Surg.* **2013**, 8, 407.
- [176] R. Reilink, S. Stramigioli, S. Misra, in *2012 IEEE Int. Conf. Robotics and Automation (ICRA)*, IEEE, Piscataway, NJ **2012**, pp. 2938–2943.
- [177] P. Cabras, D. Goyard, F. Nageotte, P. Zanne, C. Doignon, in *2014 IEEE/RSJ Int. Conf. Intell. Rob. Syst. (IROS 2014)*, IEEE, Piscataway, NJ **2014**, pp. 3522–3528.
- [178] J. Stoll, H. L. Ren, P. E. Dupont, *IEEE Trans. Med. Imaging* **2012**, 31, 563.
- [179] E. M. Boctor, M. A. Choti, E. C. Burdette, R. J. Webster, *Int. J. Med. Rob. Comput. Assisted Surg.* **2008**, 4, 180.
- [180] P. Moreira, S. Misra, *Ann. Biomed. Eng.* **2015**, 43, 1716.
- [181] P. Lang, P. Seslija, M. W. A. Chu, D. Bainbridge, G. M. Guiraudon, D. L. Jones, T. M. Peters, *IEEE Trans. Biomed. Eng.* **2012**, 59, 1444.
- [182] X. L. Wu, J. Housden, Y. L. Ma, B. Razavi, K. Rhode, D. Rueckert, *IEEE Trans. Med. Imaging* **2015**, 34, 861.
- [183] C. Kim, F. Schafer, D. Y. Chang, D. Petrisor, M. Han, D. Stoianovici, in *2011 IEEE/RSJ Int. Conf. Intelligent Robots and Systems*, IEEE, Piscataway, NJ **2011**, pp. 943–948.
- [184] A. L. Trejos, A. W. Lin, M. P. Pytel, R. V. Patel, R. A. Malthaner, *Int. J. Med. Rob. Comput. Assisted Surg.* **2007**, 3, 41.
- [185] C. Nadeau, H. L. Ren, A. Krupa, P. Dupont, *IEEE Trans. Autom. Sci. Eng.* **2015**, 12, 367.
- [186] S. B. Kesner, R. D. Howe, *IEEE Trans. Rob.* **2011**, 27, 1045.
- [187] M. Abayazid, G. J. Vrooijink, S. Patil, R. Alterovitz, S. Misra, *Int. J. Comput. Assisted Radiol. Surg.* **2014**, 9, 931.
- [188] M. Russo, S. M. H. Sadati, X. Dong, A. Mohammad, I. D. Walker, C. Bergeles, K. Xu, D. A. Axinte, *Adv. Intell. Syst.* **2023**, 5, 2200367.
- [189] D. Trivedi, A. Lotfi, C. D. Rahn, *IEEE Trans. Rob.* **2008**, 24, 773.
- [190] J. Till, V. Aloï, C. Rucker, *Int. J. Rob. Res.* **2019**, 38, 723.
- [191] M. Gazzola, L. H. Dudte, A. G. McCormick, L. Mahadevan, *R. Soc. Open Sci.* **2018**, 5, 171628.
- [192] S. M. Mustaza, Y. Elsayed, C. Lekakou, C. Saaj, J. Fras, *Soft Rob.* **2019**, 6, 305.
- [193] C. Della Santina, D. Rus, *IEEE Rob. Autom. Lett.* **2020**, 5, 290.
- [194] C. Della Santina, A. Bicchi, D. Rus, *IEEE Rob. Autom. Lett.* **2020**, 5, 1001.
- [195] I. S. Godage, E. Guglielmino, D. T. Branson, G. A. Medrano-Cerda, D. G. Caldwell, in *2011 IEEE/RSJ Int. Conf. Intelligent Robots and Systems*, IEEE, Piscataway, NJ **2011**, pp. 1093–1098.
- [196] C. Della Santina, R. K. Katschmann, A. Bicchi, D. Rus, *Int. J. Rob. Res.* **2020**, 39, 490.
- [197] A. Shiva, S. M. H. Sadati, Y. Noh, J. Fras, A. Ataka, H. Wurdemann, H. Hauser, I. D. Walker, T. Nanayakkara, K. Althoefer, *Soft Rob.* **2019**, 6, 228.
- [198] S. M. H. Sadati, S. E. Naghibi, A. Shiva, B. Michael, L. Renson, M. Howard, C. D. Rucker, K. Althoefer, T. Nanayakkara, S. Zschaler, C. Bergeles, *Int. J. Rob. Res.* **2021**, 40, 296.
- [199] F. Renda, F. Boyer, J. Dias, L. Seneviratne, *IEEE Trans. Rob.* **2018**, 34, 1518.
- [200] X. J. Huang, J. Zou, G. Y. Gu, *IEEE/ASME Trans. Mechatron.* **2021**, 26, 3175.
- [201] E. Coevoet, T. Morales-Bieze, F. Largilliere, Z. Zhang, M. Thieffry, M. Sanz-Lopez, B. Carrez, D. Marchal, O. Gouy, J. Dequidt, C. Duriez, *Adv. Rob.* **2017**, 31, 1208.



- [202] F. Renda, F. Giorgio-Serchi, F. Boyer, C. Laschi, J. Dias, L. Seneviratne, *Int. J. Rob. Res.* **2018**, *37*, 648.
- [203] P. Schegg, C. Duriez, *Plos One* **2022**, *17*, 0251059.
- [204] S. M. H. Sadati, S. E. Naghibi, I. D. Walker, K. Althoefer, T. Nanayakkara, *IEEE Rob. Autom. Lett.* **2018**, *3*, 328.
- [205] T. S. Lee, E. A. Alandoli, *J. Braz. Soc. Mech. Sci. Eng.* **2020**, *42*, 508.
- [206] C. Della Santina, R. K. Katzschmann, A. Bicchi, D. Rus, in *2018 IEEE Int. Conf. Soft Robotics (RoboSoft)*, IEEE, Piscataway, NJ **2018**, pp. 46–53.
- [207] C. Della Santina, L. Pallottino, D. Rus, A. Bicchi, *IEEE Rob. Autom. Lett.* **2019**, *4*, 2508.
- [208] M. Thieffry, A. Kruszewski, O. Goury, T.-M. Guerra, C. Duriez, *Dynamic Control of Soft Robots*, IFAC World Congress, Toulouse, France **2017**.
- [209] M. Thieffry, A. Kruszewski, T.-M. Guerra, C. Duriez, *IEEE Trans. Control Syst. Technol.* **2019**, *29*, 556.
- [210] R. K. Katzschmann, M. Thieffry, O. Goury, A. Kruszewski, T.-M. Guerra, C. Duriez, D. Rus, in *2019 2nd IEEE Int. Conf. Soft Robotics (RoboSoft)*, IEEE, Piscataway, NJ **2019**, pp. 717–724.
- [211] M. Thieffry, A. Kruszewski, C. Duriez, T.-M. Guerra, *IEEE Rob. Autom. Lett.* **2019**, *4*, 25.
- [212] G. Fang, X. Wang, K. Wang, K.-H. Lee, J. D. L. Ho, N.-C. Fu, D. K. C. Fu, K. W. Kwok, *IEEE Rob. Autom. Lett.* **2019**, *4*, 1194.
- [213] G. Zhou, J. Zhou, Y. Fang, X. Yang, *Energy* **2019**, *179*, 1082.
- [214] A. Melingui, R. Merzouki, J. B. Mbeye, C. Escande, B. Daachi, N. Benoudjit, in *Proc. Int. Joint Conf. Neural Networks*, IEEE, Piscataway, NJ **2014**, pp. 754–761.
- [215] M. Giorelli, F. Renda, M. Calisti, A. Arienti, G. Ferri, C. Laschi, *IEEE Trans. Rob.* **2015**, *31*, 823.
- [216] M. Giorelli, F. Renda, M. Calisti, A. Arienti, G. Ferri, C. Laschi, *Bioinspiration Biomimetics* **2015**, *10*, 035005.
- [217] J. Chen, H. Y. K. Lau, in *Proc. 2016 2nd Int. Conf. Control, Automation and Robotics*, IEEE, Piscataway, NJ **2016**, pp. 103–107.
- [218] T. G. Thuruthel, E. Falotico, M. Cianchetti, C. Laschi, in *ROMANSY 21 - Robot Design, Dynamics and Control*, Springer, Berlin, Heidelberg **2016**, pp. 47–54.
- [219] K.-H. Lee, D. K. C. Fu, M. C. W. Leong, M. Chow, H.-C. Fu, K. Althoefer, K. Y. Sze, C. K. Yeung, K. W. Kwok, *Soft Rob.* **2017**, *4*, 324.
- [220] W. Xu, J. Chen, H. Y. K. Lau, H. Ren, *Int. J. Med. Rob. Comput. Assisted Surg.* **2017**, *13*, e1774.
- [221] T. G. Thuruthel, E. Falotico, F. Renda, C. Laschi, *IEEE Trans. Rob.* **2019**, *35*, 124.
- [222] X. Liu, R. Gasoto, Z. Jiang, C. Onal, J. Fu, in *2020 IEEE/RSJ Int. Conf. Intelligent Robots and Systems (IROS)*, IEEE, Piscataway, NJ **2020**, p. 7758.
- [223] A. S. Polydoros, L. Nalpantidis, *J. Intell. Rob. Syst.* **2017**, *86*, 153.
- [224] X. You, Y. Zhang, X. Chen, X. Liu, Z. Wang, H. Jiang, X. Chen, in *IEEE Int. Conf. Intelligent Robots and Systems*, IEEE, Piscataway, NJ, September 2017, pp. 2909–2915.
- [225] H. Jiang, Z. Wang, Y. Jin, X. Chen, P. Li, Y. Gan, S. Lin, X. Chen, *Int. J. Rob. Res.* **2021**, *40*, 411.
- [226] S. Satheeshbabu, N. K. Uppalapati, G. Chowdhary, G. Krishnan, in *2019 Int. Conf. Robotics And Automation (ICRA)*, IEEE, Piscataway, NJ **2019**, pp. 5133–5139.
- [227] Z. Y. Wang, T. Schaul, M. Hessel, H. van Hasselt, M. Lanctot, N. de Freitas, in *Int. Conf. Machine Learning*, Vol. 48, PMLR, New York, NY, USA **2016**.
- [228] Y. Ansari, M. Manti, E. Falotico, M. Cianchetti, C. Laschi, *IEEE Rob. Autom. Lett.* **2018**, *3*, 108.
- [229] S. Satheeshbabu, N. K. Uppalapati, T. S. Fu, G. Krishnan, in *2020 3rd IEEE Int. Conf. Soft Robotics (RoboSoft)*, IEEE, Piscataway, NJ **2020**, pp. 497–503.
- [230] D. Braganza, D. M. Dawson, I. D. Walker, N. Nath, *IEEE Trans. Rob.* **2007**, *23*, 1270.
- [231] J. F. Queisser, K. Neumann, M. Rolf, R. F. Reinhart, J. J. Steil, in *IEEE Int. Conf. Intelligent Robots and Systems (IROS)*, IEEE, Piscataway, NJ **2014**, pp. 573–579.
- [232] B. Subudhi, A. S. Morris, *Appl. Soft Comput.* **2009**, *9*, 149.
- [233] Z. Q. Tang, H. L. Heung, K. Y. Tong, Z. Li, in *2019 Int. Conf. Robotics And Automation (ICRA)*, IEEE, Piscataway, NJ **2019**, pp. 4004–4010.
- [234] Z. Q. Tang, H. L. Heung, K. Y. Tong, Z. Li, *Int. J. Rob. Res.* **2021**, *40*, 256.
- [235] R. F. Reinhart, J. J. Steil, in *3rd Int. Conf. System-Integrated Intelligence: New Challenges for Product and Production Engineering*, Elsevier, Amsterdam, Netherlands **2016**, pp. 12–19.
- [236] R. F. Reinhart, Z. Shareef, J. J. Steil, *Sensors* **2017**, *17*, 311.
- [237] X. Wang, Y. Li, K.-W. Kwok, *Front. Rob. AI* **2021**, *8*, 730330.
- [238] S. Isnard, W. K. Silk, *Am. J. Bot.* **2009**, *96*, 1205.
- [239] I. Fiorello, E. Del Dottore, F. Tramacere, B. Mazzolai, *Bioinspiration Biomimetics* **2020**, *15*, 31001.
- [240] E. W. Hawkes, L. H. Blumenschein, J. D. Greer, A. M. Okamura, *Sci. Rob.* **2017**, *2*, 1.
- [241] Y. Liu, D. Wang, *J. Morphol.* **2019**, *280*, S45.
- [242] Y. W. Liu, Z. Ge, S. K. Yang, I. D. Walker, Z. J. Ju, *J. Mech. Rob.-Trans. ASME* **2019**, *11*, 051008.
- [243] R. Vidoni, T. Mimmo, C. Pandolfi, *J. Bionic Eng.* **2015**, *12*, 250.
- [244] D. Palmer, D. Axinte, *Rob. Comput. Integr. Manuf.* **2019**, *56*, 107.
- [245] A. Mohammad, M. Russo, Y. H. Fang, X. Dong, D. Axinte, J. Kell, *IEEE Rob. Autom. Lett.* **2021**, *6*, 7493.
- [246] H. El-Hussieny, U. Mehmood, Z. Mehdi, S.-G. Jeong, M. Usman, E. W. Hawkes, A. M. Okamura, J.-H. Ryu, in *2018 IEEE/RSJ Int. Conf. Intelligent Robots and Systems (IROS)*, IEEE, Piscataway, NJ **2018**, pp. 4995–5002.
- [247] D. Palmer, S. Cobos-Guzman, D. Axinte, *Rob. Auton. Syst.* **2014**, *62*, 1478.
- [248] L. Dupourque, F. Masaki, Y. L. Colson, T. Kato, N. Hata, *Int. J. Comput. Assisted Radiol. Surg.* **2019**, *14*, 2021.
- [249] Y. Q. Gao, K. Takagi, T. Kato, N. Shono, N. Hata, *IEEE Trans. Biomed. Eng.* **2020**, *67*, 379.
- [250] Y. Cao, Y. Shi, W. Hong, P. Dai, X. Sun, H. Yu, L. Xie, *Int. J. Med. Rob. Comput. Assisted Surg.* **2023**, *19*, e2471.
- [251] H. Su, C. Yang, G. Ferrigno, E. De Momi, *IEEE Rob. Autom. Lett.* **2019**, *4*, 1447.
- [252] Y. Cao, F. Feng, Z. Liu, L. Xie, in *2022 IEEE Int. Conf. Real-time Computing and Robotics (RCAR)*, IEEE, Piscataway, NJ **2022**, pp. 1–6.
- [253] T. L. Bruns, A. A. Ramirez, M. A. Emerson, R. A. Lathrop, A. W. Mahoney, H. B. Gilbert, C. L. Liu, P. T. Russell, R. F. Labadie, K. D. Weaver, R. J. Webster, *Int. J. Rob. Res.* **2021**, *40*, 521.
- [254] W. Hong, Y. Zhou, Y. Cao, F. Feng, Z. Liu, K. Li, L. Xie, *Int. J. Med. Rob. Comput. Assisted Surg.* **2022**, *18*, e2340.
- [255] W. Hong, L. Xie, J. Liu, Y. Sun, K. Li, H. Wang, *IEEE/ASME Trans. Mechatron.* **2018**, *23*, 1226.
- [256] H. Shen, C. Wang, L. Xie, S. Zhou, L. Gu, H. Xie, *Int. J. Comput. Assisted Radiol. Surg.* **2019**, *14*, 671.
- [257] H.-S. Yoon, J. H. Jeong, B.-J. Yi, *IEEE Trans. Rob.* **2018**, *34*, 1098.
- [258] J. Burgner, D. C. Rucker, H. B. Gilbert, P. J. Swaney, P. T. Russell, K. D. Weaver, R. J. Webster, *IEEE/ASME Trans. Mechatron.* **2014**, *19*, 996.
- [259] W. Hong, F. Feng, L. Xie, G.-Z. Yang, *IEEE/ASME Trans. Mechatron.* **2022**, *27*, 4440.
- [260] P. Baksic, H. Courtecuisse, B. Bayle, in *2021 IEEE Int. Conf. Robotics and Automation (ICRA)*, IEEE, Piscataway, NJ **2021**, pp. 12442–12448.
- [261] K. Song, P. Hsieh, *Asian J. Control* **2022**, *24*, 1042.

- [262] P.-L. Yen, T.-H. Ho, *IEEE Rob. Autom. Lett.* **2021**, *6*, 8394.
- [263] C. Lauretti, F. Cordella, C. Tamantini, C. Gentile, F. S. di Luzio, L. Zollo, *IEEE Rob. Autom. Lett.* **2020**, *5*, 2554.
- [264] M. W. Hannan, I. D. Walker, *J. Rob. Syst.* **2003**, *20*, 45.
- [265] L. Tang, J. Huang, L.-M. Zhu, X. Zhu, G. Gu, *IEEE/ASME Trans. Mechatron.* **2019**, *24*, 935.
- [266] T. Liu, R. Jackson, D. Franson, N. L. Poirot, R. K. Criss, N. Seiberlich, M. A. Griswold, M. Cenk Cavusoglu, *IEEE/ASME Trans. Mechatron.* **2017**, *22*, 1765.
- [267] F. Khan, A. Denasi, D. Barrera, J. Madrigal, S. Sales, S. Misra, *IEEE Sens. J.* **2019**, *19*, 5878.
- [268] N. Garbin, L. Wang, J. H. Chandler, K. L. Obstein, N. Simaan, P. Valdastrì, *IEEE Trans. Biomed. Eng.* **2019**, *66*, 1963.
- [269] K. C. Lau, E. Y. Y. Leung, P. W. Y. Chiu, Y. Yarn, J. Y. W. Lau, C. C. Y. Poon, *IEEE Trans. Ind. Inf.* **2016**, *12*, 2365.
- [270] Y. Kong, J. Wang, N. Zhang, S. Song, B. Li, *IEEE Rob. Autom. Lett.* **2022**, *7*, 8347.
- [271] E. J. Butler, R. Hammond-Oakley, S. Chawarski, A. H. Gosline, P. Codd, T. Anor, J. R. Madsen, P. E. Dupont, J. Lock, in *2012 IEEE/RSJ Int. Conf. Intelligent Robots and Systems (IROS)*, IEEE, Piscataway, NJ **2012**, pp. 2941–2946.
- [272] A. J. Chiluisa, F. J. Van Rossum, J. B. Gafford, R. F. Labadie, R. J. Webster, L. Fichera, in *2020 Int. Symp. Medical Robotics (ISMR)*, IEEE, Piscataway, NJ **2020**, pp. 188–194.
- [273] K. Wang, X. Wang, J. D.-L. Ho, G. Fang, B. Zhu, R. Xie, Y.-H. Liu, K. W. Samuel Au, J. Y.-K. Chan, K.-W. Kwok, *IEEE Trans. Rob.* **2023**, *39*, 3043.
- [274] Z. Koszowska, M. Brockdorff, T. da Veiga, G. Pittiglio, P. Lloyd, T. Khan-White, R. A. Harris, J. W. Moor, J. H. Chandler, P. Valdastrì, *Adv. Intell. Syst.* **2023**, 2300062.
- [275] W. Li, D. Zhang, G.-Z. Yang, B. Lo, in *2022 IEEE/RSJ Int. Conf. Intelligent Robots and Systems (IROS)*, IEEE, Piscataway, NJ **2022**, pp. 41–47.
- [276] Z. Hu, J. Li, S. Wang, *IEEE/ASME Trans. Mechatron.* **2023**, *28*, 2840.
- [277] C. Li, X. Gu, X. Xiao, C. M. Lim, H. Ren, *Med. Biol. Eng. Comput.* **2020**, *58*, 2063.
- [278] N. Garbin, L. Wang, J. H. Chandler, K. L. Obstein, N. Simaan, P. Valdastrì, in *2018 Int. Symp. Medical Robotics (ISMR)*, IEEE, Piscataway, NJ **2018**.
- [279] Q. Jacquemin, Q. Sun, D. Thuau, E. Monteiro, S. Tence-Girault, N. Mechbal, in *2020 IEEE/RSJ Int. Conf. Intelligent Robots and Systems (IROS)*, IEEE, Piscataway, NJ **2020**, pp. 3208–3215.
- [280] D. Kundrat, R. Graesslin, A. Schoob, D. T. Friedrich, M. O. Scheithauer, T. K. Hoffmann, T. Ortmaier, L. A. Kahrs, P. J. Schuler, *Ann. Biomed. Eng.* **2021**, *49*, 585.
- [281] D. Kundrat, A. Schoob, T. Piskon, R. Grässlin, P. J. Schuler, T. K. Hoffmann, L. A. Kahrs, T. Ortmaier, *IEEE Trans. Med. Rob. Bionics* **2019**, *1*, 145.
- [282] X. Zhang, W. B. Li, W. Y. Ng, Y. S. Huang, Y. T. Xian, P. W. Y. Chiu, Z. Li, in *2021 IEEE Int. Conf. Robotics And Automation (ICRA 2021)*, IEEE, Piscataway, NJ **2021**, pp. 12055–12060.
- [283] Y. Chen, J. H. Liang, I. W. Hunter, in *2014 IEEE Int. Conf. Robotics and Automation (ICRA)*, IEEE, Piscataway, NJ **2014**, pp. 5393–5400.
- [284] A. Z. Gao, N. Liu, H. J. Zhang, Z. C. Wu, G. Z. Yang, *Biosens. Bioelectron.* **2020**, *170*, 112653.
- [285] Z. Yin, Y. Hong, X. Sun, Z. Shen, Y. Zhang, F. Ju, B. W. Drinkwater, in *2022 IEEE/RSJ Int. Conf. Intelligent Robots and Systems (IROS)*, IEEE, Piscataway, NJ **2022**, pp. 5945–5950.
- [286] T. Kato, I. Okumura, S. E. Song, A. J. Golby, N. Hata, *IEEE/ASME Trans. Mechatron.* **2015**, *20*, 2252.
- [287] T. Kato, I. Okumura, H. Kose, K. Takagi, N. Hata, in *2014 IEEE/RSJ Int. Conf. Intelligent Robots and Systems (IROS 2014)*, IEEE, Piscataway, NJ **2014**, pp. 1997–2002.
- [288] T. Kato, I. Okumura, S. E. Song, N. Hata, in *Medical Image Computing and Computer-Assisted Intervention (MICCAI 2013)*, *PT I*, 8149, Springer, Berlin, Heidelberg **2013**, pp. 364–371.
- [289] X. M. Ye, Y. Z. Gong, W. J. Yoon, *IEEE/ASME Trans. Mechatron.* **2016**, *21*, 993.
- [290] Q. P. Ding, Y. K. Lu, A. Kyme, S. S. Cheng, in *2021 IEEE Int. Conf. Robotics and Automation (ICRA 2021)*, IEEE, Piscataway, NJ **2021**, pp. 11930–11937.
- [291] Q. H. Guan, J. Sun, Y. J. Liu, N. M. Wereley, J. S. Leng, *Soft Rob.* **2020**, *7*, 597.
- [292] B. Q. Su, M. D. Jin, H. C. Wu, L. L. Liu, H. Liu, J. N. Wang, H. Sun, L. Lam, Y. Li, in *2019 World Robot Conf. Symp. Advanced Robotics and Automation (WRC SARA 2019)*, IEEE, Piscataway, NJ **2019**, pp. 44–49.
- [293] F. Masaki, F. King, T. Kato, H. Tsukada, Y. Colson, N. Hata, *IEEE Trans. Biomed. Eng.* **2021**, *68*, 3534.
- [294] B. Wu, C. Zhou, X. Wang, D. Sun, K. Xu, *Sci. China Technol. Sci.* **2023**, *66*, 2517.
- [295] A. Kuntz, M. Fu, R. Alterovitz, in *2019 IEEE/RSJ Int. Conf. Intelligent Robots and Systems (IROS)*, IEEE, Piscataway, NJ **2019**, pp. 2205–2212.
- [296] Z. Wang, T. Wang, B. Zhao, Y. He, Y. Hu, B. Li, P. Zhang, M. Q. H. Meng, *IEEE Rob. Autom. Lett.* **2021**, *6*, 1407.
- [297] Y. Zhong, L. H. Hu, Y. S. Xu, *Actuators* **2020**, *9*, 142.
- [298] S. Y. Li, G. B. Hao, *Actuators* **2021**, *10*, 145.
- [299] Z. X. Yang, H. J. Yang, Y. F. Cao, Y. Y. Cui, L. Zhang, *Adv. Intell. Syst.* **2023**, *5*, 2200416.
- [300] FANUC America Corporation, (2023). *M-1000iA Industrial Robot* <https://www.fanucamerica.com/products/robots/series/m-1000ia> **2023**.
- [301] B. Mazzolai, A. Mondini, F. Tramacere, G. Riccorni, A. Sadeghi, G. Giordano, E. Del Dottore, M. Scaccia, M. Zampato, S. Carminati, *Adv. Intell. Syst.* **2019**, *1*, 1900041.
- [302] T. L. de Jong, N. J. van de Berg, L. Tas, A. Moelker, J. Dankelman, J. J. van den Dobbelsteen, *Med. Devices: Evidence Res.* **2018**, *11*, 259.
- [303] J. Tian, *Research on the Key Technologies of Continuum Robot for Aero-Engine Borescopic Inspection*, Beihang University, Beijing, China **2021**, p. 2021.
- [304] A. Marmol, P. Corke, T. Peynot, in *2018 IEEE/RSJ Int. Conf. Intelligent Robots and Systems (IROS)*, IEEE, Piscataway, NJ **2018**, pp. 3882–3889.
- [305] A. Marmol, A. Banach, T. Peynot, *IEEE Rob. Autom. Lett.* **2019**, *4*, 918.
- [306] C.-K. Kim, J. Kim, D. Park, D.-S. Kwon, *IEEE Access* **2021**, *9*, 27416.
- [307] J. W. Suh, K. Y. Kim, J. W. Jeong, J. J. Lee, *IEEE/ASME Trans. Mechatron.* **2015**, *20*, 2841.
- [308] Z. Li, M. Z. Oo, V. Nalam, V. D. Thang, H. L. Ren, T. Kofidis, H. Yu, *J. Mech. Rob.* **2016**, *8*, 051014.
- [309] Y. Zhang, H. Sun, Y. Jia, D. Huang, R. Li, Z. Mao, Y. Hu, J. Chen, S. Kuang, J. Tang, X. Xiao, B. Su, in *2018 IEEE 14th Int. Conf. Control and Automation (ICCA)*, IEEE, Piscataway, NJ **2018**, pp. 1150–1155.



**Tengbo Yu** is a chief physician and working as a professor in the University of Health and Rehabilitation Science affiliated Qingdao Municipal Hospital. Currently, he serves as the president of Qingdao Municipal Hospital. Additionally, he is a member of the Sports Medicine Branch and Orthopedic Branch of the Chinese Medical Association and the Chinese Medical Doctor Association, and he holds the position of Vice Chairman of the Orthopedic Branch. He has authored over 270 professional papers, including more than 70 papers in SCI and Chinese core journals as the first author or corresponding author. He has declared 34 national patents, of which 21 have been authorized.



**Chaozog Liu** is a Professor and Director of Centre for Bioengineering & Surgical Technology at University College London, UCL Institute of Orthopedics and Musculoskeletal Science. His research is directed toward biomaterials innovation for orthopedic applications with particular emphasis on the early diagnosis and early treatment of musculoskeletal disorders. His research in this area is supported by Versus Arthritis UK, Innovate UK, Horizon2020, NIHR, EPSRC, and MRC.